

DESIGN AND DEVELOPMENT OF MODIFIED SEPIC CONVERTER FOR BLDC DRIVE



A PROJECT REPORT

Submitted by

ASWIN C. (1903016)
GIRIPRASATH M.U. (1903026)
HARIHARAN B. (1903032)

in partial fulfillment for the award of the degree of

BACHELOR OF ENGINEERING

in

ELECTRICAL AND ELECTRONICS ENGINEERING

SRI RAMAKRISHNA ENGINEERING COLLEGE

(AN AUTONOMOUS INSTITUTION)

COIMBATORE – 641 022

ANNA UNIVERSITY::CHENNAI 600 025

APRIL 2023

ANNA UNIVERSITY : CHENNAI 600 025

BONAFIDE CERTIFICATE

Certified that this project report titled "**DESIGN AND DEVELOPMENT OF MODIFIED SEPIC CONVERTER FOR BLDC DRIVE**" is the bonafide work of "**ASWIN C., GIRIPRASATH M.U. and HARIHARAN B.**" who carried out the project work under my supervision.

SIGNATURE

Dr.S.Allirani

HEAD OF THE DEPARTMENT*i/c*

Associate Professor,
Electrical and Electronics Engineering,
Sri Ramakrishna Engineering College ,
Vattamalaipalayam,
N.G.G.O.Colony Post,
Coimbatore – 641022.

SIGNATURE

Mr.C.Praveenkumar

SUPERVISOR

Assistant Professor (Sr.G),
Electrical and Electronics Engineering,
Sri Ramakrishna Engineering College,
Vattamalaipalayam,
N.G.G.O.Colony Post,
Coimbatore – 641022.

Submitted for the Project Viva-Voce Examination held on _____

INTERNAL EXAMINER

EXTERNAL EXAMINER

ACKNOWLEDGEMENT

We put forth our hearts and souls to thank the ALMIGHTY for being with us through our achievements and success. We would like to express our unfathomable thanks to our esteemed and Honorable Managing Trustee **Sri D.Lakshminarayanaswamy** and Joint Managing Trustee **Sri R.Sundar** for giving us the chance to be a part of this elite team at Sri Ramakrishna Engineering College, Coimbatore.

We would like to express our sincere thanks to our honorable Principal, **Dr.N.R.Alamelu** for her continuous motivation towards the development of the students.

We take the privilege to thank the Associate Professor and Head of the Department In-Charge of Electrical and Electronics Engineering, **Dr.S.Allirani** for her consistent support and encouragement at every step of our project work.

We would like to express our sincere thanks to our project coordinators, **Dr.P.Sebastian Vindro Jude** and **Mr.C.Praveenkumar**, Assistant Professors/Department of Electrical and Electronics Engineering for their valuable support during the course of development and completion of this project.

We wish to convey our special thanks to our project supervisor, **Mr.C.Praveenkumar** Assistant Professor (Senior Grade), Department of Electrical and Electronics Engineering for his consistent support, timely help and valuable suggestions during the entire period of our project work.

We extend our sincere gratitude to all the teaching and non-teaching staff members of our department who helped us during our project.

We express heartfelt gratitude to our parents for bringing us into this world, inspiring us, standing by us, and providing us with a valuable education that enabled us to successfully completing our project to earn our degree.

ABSTRACT

A system to work properly needs a suitable DC-DC converter. High output voltage and power, low harmonic distortion, low ripple content at both current and voltage, and high efficiency gain with fewer component requirements are just a few of the parameters for a good converter. Such types of converters are need to be designed to meet some of the aforementioned requirements. With increased potential for BLDC drive based Electric Vehicle (EV) applications, the converter chosen for this project is a type of DC-DC converter (said Modified SEPIC) that will be suitable for high power rating of applications. Before recommending a converter for a certain usage, its performance must be evaluated. The validation process goes into great detail for the design topology, components used, equations created, loss calculations, and output performances. The majority of converters perform better than expected, when choosing the right component values. Applications that work well are provided together with the findings of the converters and the related values. Upon considering the performance of various converters it is proven that Modified SEPIC converter produces output voltage and output current as 41.2v and 41.12A respectively. It is 1.99 times for the voltage conversion ratio, the output ripple is observed as 0.30% with an efficiency of 73.8%.

ஆய்வுச்சுருக்கம்

ஒரு கருவி சரியாக வேலை செய்ய பொருத்தமான DC-DC மின்மாற்றி தேவை. அதிக வெளியீட்டு மின்னழுத்தம் மற்றும் சக்தி, குறைந்த ஹார்மோனிக் விலகல், மின்னோட்டம் மற்றும் மின்னழுத்தம் இரண்டிலும் குறைந்த சிற்றலை உள்ளடக்கம் மற்றும் குறைவான கூறு தேவைகளுடன் கூடிய உயர் செயல்திறன் ஆதாயம் ஆகியவை ஒரு நல்ல மாற்றிக்கான அளவுருக்களில் சில. மேற்கூறிய சில தேவைகளைப் பூர்த்தி செய்யும் வகையில் இத்தகைய மின்மாற்றிகள் வடிவமைக்கப்பட வேண்டும். BLDC இயக்கி அமைப்பு அடிப்படையிலான மின்சார வாகன பயன்பாடுகளுக்கான அதிக சாத்தியக்கூறுகளுடன், இந்த கட்டுரையில் தேர்ந்தெடுக்கப்பட்ட மாற்றியானது DC-DC மின்மாற்றியின் வகையாகும் (மாற்றியமைக்கப்பட்ட SEPIC) இது பயன்பாடுகளின் உயர் ஆற்றல் மதிப்பீட்டிற்கு ஏற்றதாக இருக்கும். ஒரு குறிப்பிட்ட பயன்பாட்டிற்கு மின் மாற்றியை பரிந்துரைக்கும் முன், அதன் செயல்திறன் மதிப்பீடு செய்யப்பட வேண்டும். சரிபார்ப்பு செயல்முறை வடிவமைப்பு இடவியல், பயன்படுத்தப்படும் கூறுகள், உருவாக்கப்பட்ட சமன்பாடுகள்,

இழப்பு கணக்கீடுகள் மற்றும் வெளியீட்டு செயல்திறன் ஆகியவற்றிற்கு மிகவும் விரிவாக செல்கிறது. சரியான கூறு மதிப்புகளைத் தேர்ந்தெடுக்கும்போது, பெரும்பாலான மின்மாற்றிகள் எதிர்பார்த்ததை விட சிறப்பாகச் செயல்படுகின்றன. நன்றாக வேலை செய்யும் பயன்பாடுகள் மின் மாற்றிகளின் கண்டுபிடிப்புகள் மற்றும் தொடர்புடைய மதிப்புகளுடன் வழங்கப்படுகின்றன. பல்வேறு மின்மாற்றிகளின் செயல்திறனைக் கருத்தில் கொண்டு, மாற்றியமைக்கப்பட்ட SEPIC மின் மாற்றியானது வெளியீட்டு மின்னழுத்தம் மற்றும் வெளியீட்டு மின்னோட்டத்தை முறையே 41.2v மற்றும் 41.12A ஆக உருவாக்குகிறது என்பது நிரூபிக்கப்பட்டுள்ளது. மின்னழுத்த மாற்ற விகிதத்திற்கு இது 1.99 மடங்கு ஆகும், வெளியீட்டு சிற்றலை 73.8% செயல்திறனுடன் 0.30% ஆகக் காணப்படுகிறது.

TABLE OF CONTENTS

CHAPTER NO	TITLE	PAGE NO
	ABSTRACT – ENGLISH	iv
	ABSTRACT – TAMIL	v
	TABLE OF CONTENTS	vii
	LIST OF TABLES	xi
	LIST OF FIGURES	xii
	LIST OF ABBREVIATION	xiii
1	INTRODUCTION	1
	1.1 GENERAL INTRODUCTION	1
	1.2 PROPOSED BLOCK DIAGRAM	4
	1.3 EXISTING SEPIC CONVERTER	5
	1.4 PROPOSED MODIFIED SEPIC CONVERTER	7
	1.5 ZETA CONVERTER	9
	1.6 CUK CONVERTER	11
	1.7 QUASI Z-SOURCE CONVERTER	13
	1.8 OBJECTIVE OF THE PROJECT	15
	1.9 ORGANISATION OF THE REPORT	15
2	LITERATURE SURVEY	17
	2.1 POWER FACTOR CORRECTION IN CUK–SEPIC-BASED DUAL-OUTPUT-CONVERTER-FED SRM DRIVE	17
	2.2 POWER FACTOR CORRECTION IN BRIDGELESS-LUO CONVERTER FED BLDC MOTOR DRIVE	17

2.3	BRIDGELESS PFC MODIFIED SEPIC RECTIFIER WITH EXTENDED GAIN FOR UNIVERSAL INPUT VOLTAGE APPLICATIONS	18
2.4	MODIFIED ISOLATED POWER FACTOR CORRECTION CUK- CONVERTER FED BLDC MOTOR DRIVE WITH FUZZY LOGIC CONTROLLER FOR PUMPING APPLICATIONS	18
2.5	FUZZY AND PID CONTROLLERS FOR BUCK- BOOST CONVERTER FED BRIDGELESS BLDC MOTOR OVER CLOUD	19
2.6	CONTROL AND ANALYSIS OF BIDIRECTIONAL INTERLEAVED HYBRID CONVERTER WITH COUPLED INDUCTORS FOR ELECTRIC VEHICLE APPLICATIONS	19
2.7	INTERLEAVED BIDIRECTIONAL DC-DC CONVERTER FOR ELECTRIC VEHICLE APPLICATIONS BASED ON MULTIPLE ENERGY STORAGE DEVICES	20
3	DESIGN CONSIDERATION OF CONVERTER TOPOLOGIES	21
3.1	DESIGN EQUATION OF MODIFIED SEPIC CONVERTER	21
3.2	DESIGN EQUATION OF ZETA CONVERTER	22
3.3	DESIGN EQUATION OF CUK CONVERTER	23
3.4	DESIGN EQUATION OF QUASI Z-SOURCE CONVERTER	24
4	SIMULATION AND PERFORMANCE ANALYSIS FOR THE PROPOSED CONVERTER AND THE AFOREMENTIONED CONVERTERS	26

4.1	OUTPUT RESPONSE AFOREMENTIONED CONVERTERS	26
4.1.1	MODIFIED SEPIC CONVERTER	26
4.1.2	ZETA CONVERTER	27
4.1.3	CUK CONVERTER	28
4.1.4	QUASI Z-SOURCE CONVERTER	29
4.2	COMPARISON RESULTS BETWEEN THE PROPOSED CONVERTER AND VARIOUS CONVERTERS	30
4.3	OUTPUT VOLTAGE OBTAINED FROM DIFFERENT CONVERTER TOPOLOGIES	31
5	EXPERIMENTAL ANALYSIS	34
5.1	PROTOTYPE PARAMETER	34
5.1.1	INDUCTOR	34
5.1.2	CAPACITOR	35
5.1.3	MOSFET AND GATE DRIVER	37
5.1.4	DIODE	40
5.1.5	PIC MICROCONTROLLER	42
6	CONCLUSION AND FUTURE SCOPE	45
6.1	CONCLUSION	45
6.2	FUTURE SCOPE	45
APPENDICES		46
APPENDIX 1:	MATLAB CIRCUIT	46
APPENDIX 2:	SNAPSHOT OF THE PROPOSED CONVERTER	47
APPENDIX 3:	DATASHEETS	48
REFERENCES		61

LIST OF TABLES

TABLE NO	DESCRIPTION	PAGE NO
3.1	Specifications of Modified SEPIC Converter	22
3.2	Specifications of Zeta Converter	23
3.3	Specifications of Cuk Converter	24
3.4	Specifications of Quasi Z-source Converter	25
4.1	Comparative Analysis between the Converter Topologies	33
4.2	Comparative Analysis on Efficiency and Voltage Gain	33

LIST OF FIGURES

FIG. NO.	TITLE	PAGE NO
1.1	General Block Diagram of BLDC Drive	4
1.2	SEPIC Converter's Circuit Diagram	7
1.3	Modified SEPIC Converter's Circuit Diagram	8
1.4	Zeta Converter's Circuit Diagram	11
1.5	Cuk Converter's Circuit Diagram	13
1.6	Quasi Z-Source Converter's Circuit Diagram	15
4.1	Output Response of Modified SEPIC Converter	26
4.2	Output Response of Zeta Converter	27
4.3	Output Response of Cuk Converter	28
4.4	Output Response of Quasi Z-Source Converter	29
4.5	Output Voltage Ripple Analysis	31
4.6	Input Current Ripple Analysis	32
4.7	Output Current Ripple Analysis	32
5.1	Coupled Inductor	34
5.2	Capacitor	36
5.3	MOSFET	37
5.4	FAN7392N Gate Driver IC	39
5.5	Diode	38
5.6	16F877A Microcontroller	40

LIST OF ABBREVIATION

ABBREVIATION	EXPANSION
AC	Alternate Current
BLDC	Brushless Direct Current Motor
CCM	Continuous Conduction Mode
CL	Coupled Inductor
CLBC	Coupled Inductor Boost Converter
DC	Direct Current
ESR	Equivalent Series Resistance
KVL	Kirchoff's Voltage Law
MOSFET	Metal Oxide Semiconductor Field Effect Transistor
SRM	Switched Reluctance Motor
PMAC	Permanent Magnet Alternating Current
QRO	Quasi Resonant Operation
SEPIC	Single Ended Primary Inductor Converter
SLBC	Single Inductor Boost Converter
VM	Voltage Multiplier
VMR	Voltage Multiplier Rectifier
VL	Voltage Lifts
ZCS	Zero Current Switching
ZVS	Zero Voltage Switching
PMAC	Permanent Magnet Alternating Current
PFC	Power Factor Correction
VSI	Voltage Source Inverter

CHAPTER 1

INTRODUCTION

CHAPTER 1

INTRODUCTON

This chapter explains about General introduction of the DC-DC converters for BLDC drive system, Block diagram of the proposed system and Case studies on various converter topology on comparison for following various converter topology are SEPIC converter (Existing system), Modified SEPIC converter (Proposed system), Zeta converter, Cuk converter and Quasi Z-source converter.

1.1 GENERAL INTRODUCTON

A lot of research is presently being done in order to create a sustainable DC to DC converter for use in Electric Vehicle (EV) applications. In the 1890s, the first electric vehicle emerged. However, throughout the past century, major efforts have been made to improve performance control in order to complete the adoption of EVs in the automotive sector. This research also focuses on the controlling performance improvement of EVs using batteries. The majority of EV components include an energy storage system, a motor, converter topologies, and control schemes. The motors used in electric vehicle applications include the Induction Motor (IM), Synchronous Motor (SM), Switched Reluctance Motor (SRM), DC motor, and Brush-Less DC (BLDC) Motor. Brushless DC (BLDC) motors are widely used today due to their increased performance and reduced maintenance requirements. These motors are available in different power classes, from small motors for hard drives to large motors for electric vehicles, actuators, robotics, etc. Self-driven frequency converter with PMAC (permanent magnet alternating current) sine wave motor drives brushless DC motor. Brushless DC motor drives have the advantage are maintenance-free and having a long service life. It also has a lower frequency, lower inertia and friction, and lower radio frequency interference and noise. The only drawbacks of the drive are its high cost and low starting torque. The advantages of brushless motors over brushed motors are higher power-to-weight ratio, higher speed, electronic control, and less maintenance. Among these motors, the IM and SM have some efficiency limitations, while the SRM and DC motor causes sparking and acoustic noise, respectively. The

motors discussed above have the following benefits over BLDC. It has a high power density, a strong starting torque, enhanced speed-torque characteristics, no acoustic noise or sparking, no winding on the rotary part, up to a 95% efficiency rate, and other benefits. So it makes sense to use a BLDC motor in electric vehicles. Extruder drive motors, actuators for industrial robots, feed drives for CNC machine tools, and linear and servo motors in the industrial field are further applications for BLDC motors. The following is a summary of the literature survey on selection converters. An SRM drive with a PFC-based converter combines Cuk and SEPIC converters. The SRM drive is commonly powered by a basic diode bridge rectifier, which draws peaky current with a low power factor and a high input-current THD. The next component is a sizable capacitor. The drawbacks include acoustic noise and having extra components. Power Factor Correction (PFC)-based Bridge-Less Luo (BL-Luo) converter-based BLDC motor drive was presented in One voltage sensor is used for the BLDC motor and PFC at ac mains speed control. The voltage follower control is used with a BL-Luo converter that is operating in the discontinuous inductor current mode. Because it permits low-frequency switching of the voltage source inverter for the motor's electronic commutation and lowers switching losses, a method of variable dc-link voltage is employed to control the BLDC motor's speed.

The suggested BLDC motor drive is designed to operate with better ac mains power quality and a range of speeds. A new single-phase AC-DC PFC bridgeless rectifier with a multiplier stage was invented in with the goal of improving efficiency at low input voltage and reducing switch-voltage stress. To achieve an input current with a nearly unity power factor and minimum Total Harmonic Distortion (THD), the recommended architecture was designed to operate in Discontinuous Conduction Mode (DCM). The efficiency, THD, and power factor of a modified full-bridge SEPIC rectifier were evaluated using the architecture that was demonstrated. A modified Power Factor Correction Cuk Converter (PFCCC)-operated Voltage Source Inverter (VSI)-fed BLDC motor drive was developed in for agricultural water pumping applications. To boost efficiency and PF and decrease the consequences of

the system's low PF, PFC circuits are added to the AC input side of the water pumping system. Power Factor Correction (PFC) converters, such as the Zeta DC-DC converter in are used to modify voltage to alter the speed of Permanent Magnet Brush-Less DC Motors (PMBLDCM). The recommended drive's detailed design, modelling, and performance are shown for an air conditioner using a PMBLDC motor rated at 0.817 kW and 1500 rpm. A novel bidirectional interleaved hybrid converter using linked Coupled Inductors (CIs) was proposed in in order to maximise the performance of the power train in battery electric vehicles (BEVs). Realize the integration of the DC/DC converter and DC-AC inverter in the BEV power train, acting as a backup generator to send emergency power straight to the home, with good performance in every operating mode. It can lower system costs and volume while boosting effectiveness and dependability. The interleaving structure is used in this case to increase output power, minimise input current and output voltage ripple, reduce power loss, and increase efficiency. The use of CIs of energy storage inductors enhances the performance of the proposed converter.

Supercapacitors (SCs) and batteries may be used in an EV design to deliver dependable and quick energy transfer, as discussed in Power is moved between the abovementioned energy sources and the EV via a DC link coupled to a bidirectional interleaved DC-DC converter. The converter is investigated statistically and qualitatively, and as part of a comprehensive design process, a simple control system implementation is provided. A brand-new boost-based DC-DC converter without a transformer was proposed in study by Utilizing n levels of voltage multiplier cells and a charge-pump circuit (CPC), the voltage gain of the proposed converter was increased (VMC). By building a lab prototype with a power of 300 W, input and output voltages of 30V and 310V, respectively, and a switching frequency of 40 kHz, the performance of the converter is confirmed. The hybrid converter topology, also known as the SEPIC converter fed three-level Neutral-Point-Clamped (NPC) inverter topology, was developed to eliminate torque ripples. The outcomes of this study led to the development of a system that, as detailed significantly reduces torque ripple

when compared to a system based on a two-level NPC inverter. Identifying 2-kW BLDC-based EV applications with low ripple and high current output is the main objective of this work. The outcomes of several converter topologies' simulations are then contrasted. According to Modified SEPIC results, they are quite competitive with other converters. The rest of the proposed system is structured as follows Output and reasons are presented after component design equations, simulated values, and design studies of various converter topologies. The proposed system discusses ripple content and comparative analysis. Fig.1.1 Displays the basic building blocks of the suggested approach.

1.2 PROPOSED BLOCK DIAGRAM

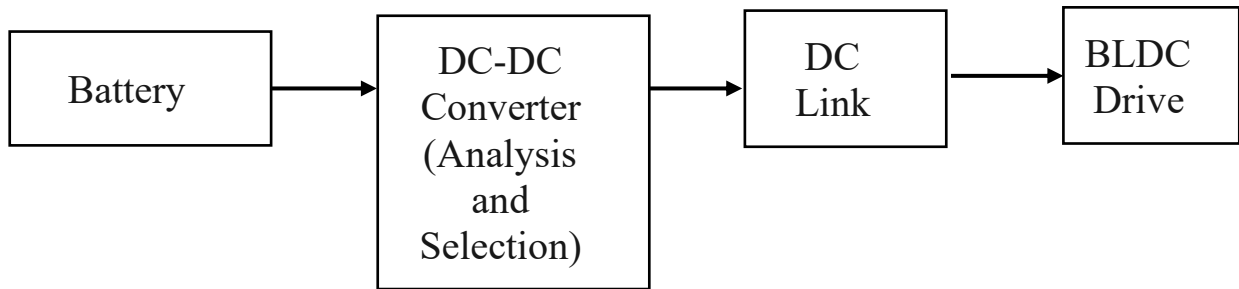


Fig. 1.1 General Block Diagram of BLDC Drive

The analysis begins with the output voltage obtained from a 24 volt battery supply then DC-DC converter takes the voltage from a DC source and converts the voltage of supply into another DC voltage level. They are used to decrease or increase the voltage level based on the drive system. A DC-DC converters use high switching frequency and inductors, transformers and capacitors to smooth out switching noise. The DC-DC converter plays a major role in determining the performance of the motor. For a BLDC motor, the switched mode regulation is provided by DC-DC converter. A DC-DC converter is the one that converts the unregulated voltage to the regulated DC voltage. after that DC link is typically composed of a capacitor or a battery that is used to store energy and provide a stable voltage source for the connected components. The capacitor is charged by the input DC source, and the stored energy is then used to provide a smooth DC voltage to the load or output. The DC link

capacitor can also help to filter out any ripple in the input voltage. And it ensures there will no wastage in power and give to BLDC drive. Here the main objective is to compare, analysis with various converters which have different types of DC-DC converter are Modified SEPIC converter, Zeta converter, Cuk converter, Quasi-z source converter. Among these converters Modified SEPIC converter is the proposed converter for these system, it will be compared with highest potential with other converters, analyzed and selected in various criteria such as High efficiency, low ripple current and voltage, minimal voltage gain, reduced in switching losses and it shows Modified SEPIC converter is suitable for BLDC drive system.

1.3 EXISTING SEPIC CONVERTER

The SEPIC converter (Single-Ended Primary Inductance Converter) is a type of non-isolated converter, which means that there is no galvanic isolation between the input and output sides of the circuit. However, isolated versions of the SEPIC converter are available for applications that require galvanic isolation. In terms of efficiency, the SEPIC converter can achieve efficiencies of up to 95% under optimal conditions. However, the efficiency of the converter may be lower under certain operating conditions, such as when the input voltage is much higher or lower than the output voltage. In switching power supplies (especially DC-DC converters), SEPICs convert one voltage to another by exchanging energy between a capacitor and an inductor. The amount of energy exchanged is controlled by switch S1. Switch S1 is typically a transistor such as a MOSFET. The MOSFETs offer much higher input impedance and lower voltage drop than Bipolar Junction Transistors (BJTs), and do not require bias resistors because MOSFET switching is controlled by a voltage difference rather than current as in BJTs. The SEPIC converter is a popular choice for LED lighting applications because it can provide a constant current output, which is necessary for driving LEDs. Additionally, the non-inverted output voltage of the SEPIC converter allows for simpler LED dimming control. The SEPIC converter is also known as the "buck-boost" converter because it can perform both step-down (buck) and step-up (boost) voltage conversion. One of the key advantages of the

SEPIC converter is its ability to regulate the output voltage even when the input voltage varies over a wide range. This makes it useful in applications where the input voltage may be subject to fluctuations or where the input voltage must be drawn from a non-ideal source, such as a battery. It uses a combination of inductors, capacitors, and diodes to step up or step down the input voltage, and has the advantage of providing a non-inverted output voltage, which is useful in many applications. SEPIC converters are commonly used in LED lighting, portable electronic devices, and automotive electronics. Fig.1.2 displays the SEPIC topology's circuit configuration. The single-ended primary-inductance converter provides a positive regulated output voltage from an input voltage that varies from above to below the output voltage. This type of conversion is handy when the designer uses voltages from an unregulated input power supply such as a low-cost wall wart.

Unfortunately, the SEPIC topology is difficult to understand and requires two inductors, making the power-supply footprint quite large. Recently, several inductor manufacturers began selling off-the-shelf coupled inductors in a single package at a cost only slightly higher than that of the comparable single inductor. The coupled inductor not only provides a smaller footprint but also, to get the same inductor ripple current, requires only half the inductance required for a SEPIC with two separate inductors. The single-ended primary-inductor topology allows the electrical potential (voltage) at its output to be greater than, less than, or equal to that at its input. The output of the SEPIC is controlled by the duty cycle of the control switch. Essentially similar to a traditional buck-boost converter, but with three primary advantages. It has a non-inverted output (the output has the same voltage polarity as the input), uses a series capacitor to couple energy from the input to the output (and thus can respond more gracefully to a short-circuit output), and is capable of true shutdown.

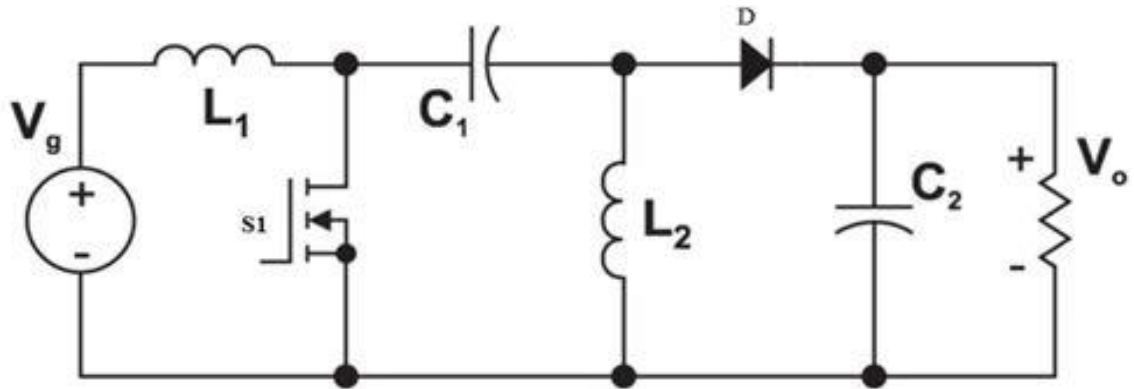


Fig. 1.2 SEPIC Converter's Circuit Diagram

1.3 PROPOSED MODIFIED SEPIC CONVERTER

A Modified SEPIC (Single-Ended Primary Inductor Converter) is also a type of DC-DC converter used to increase or decrease the voltage of a DC power supply. Unlike traditional SEPIC converters that have a single coupled inductor, the modified SEPIC uses two separate inductors instead. Modified SEPIC consists of coupled inductor, leakage inductor L1, magnetizing inductor L2, four MOSFET switch S1-S4, two intermediate capacitors C1 and C4, output capacitor C2 and C3 and load resistor R. Fig. 1.3 displays the Modified SEPIC topology's circuit configuration. The modified SEPIC topology is similar to the traditional SEPIC topology but uses two inductors to increase efficiency and reduce output voltage ripple. The two inductors are connected in parallel and the converter output is taken from the midpoint of the two inductors. Input voltage is applied to the primary side of one inductor and the other inductor is used to transfer energy to the output circuit. The main advantage of the modified SEPIC is that it allows higher voltage conversion ratios and better efficiency than conventional SEPIC, especially at high power levels. Additionally, using two separate inductors not only reduces converter size and cost, but also improves thermal performance. Overall, the modified SEPIC is a useful topology for a wide range of DC-DC converter applications such as renewable energy systems, telecommunications, and industrial control systems. In the case of High efficiency The use of two separate inductors in a modified SEPIC converter results in lower conduction losses and higher efficiency compared to traditional SEPIC converters.

This is especially true at high power levels and high voltage conversion ratios. In case of Ripple Reduction The modified SEPIC converter also offers lower output voltage ripple than his conventional SEPIC converter. This is because two inductors are used to reduce output voltage ripple. In the case of Superior thermal performance with two inductors connected in parallel, the modified SEPIC converter can distribute power more evenly, improve thermal performance and lower operating temperature.

This is especially important in high power applications where heat dissipation is a critical issue. In the case of Reduced part size Using two separate inductors reduces the overall size and cost of the converter. This is because the inductors can be optimized for their function, improving performance and reducing cost. In the case of High voltage conversion ratio Improved SEPIC converters are capable of high voltage conversion ratios, making them ideal for applications requiring voltage step-up or step-down conversion. The Modified SEPIC applications are high power, high current and static gain applications.

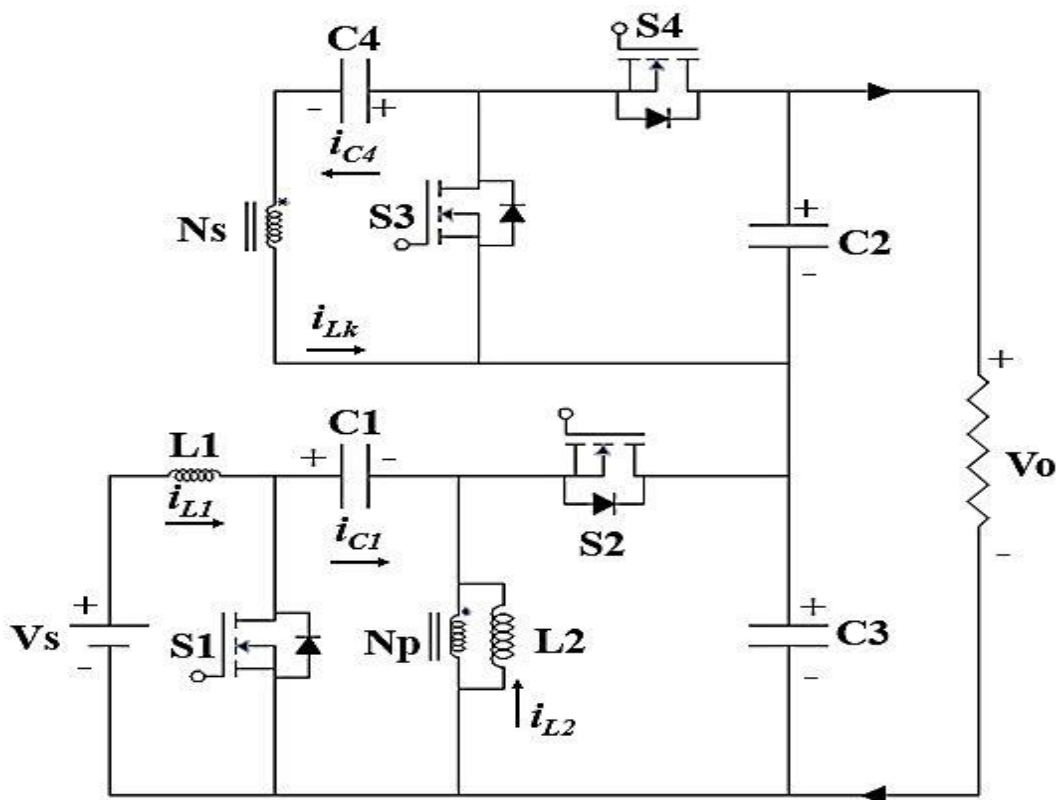


Fig. 1.3 Modified SEPIC Converter's Circuit Diagram

1.4 ZETA CONVERTER

A zeta converter is a type of power electronics converter that combines the characteristics of a buck-boost converter and a forward converter to provide high voltage gain with a single power switch. It is commonly used in applications such as telecom power supplies, industrial controls, and lighting systems. The zeta converter topology is similar to that of the SEPIC converter (single-ended primary inductance converter), but with an additional inductor and capacitor in the output stage. Zeta converters are non-isolated DC-DC converters. That is, no galvanic isolation is provided between input and output. It works by controlling a switch to alternately connect and disconnect the input voltage to the inductor and use the energy stored in the inductor to transfer energy to the output capacitor and load. One of the advantages of zeta converters is the ability to achieve high voltage gains with a single power switch. This makes it more efficient and cheaper than other DC-DC converter topologies that require multiple switches and more complex control circuits. However, zeta converters also have some of these drawbacks as they need for careful design to ensure stability and avoid voltage spikes, and the potential for electromagnetic interference (EMI) due to the use of high frequency circuits.

Overall, the zeta converter is a convenient and versatile DC-DC converter topology that can provide high voltage gain and efficient power transfer in a variety of applications using a capacitor to transfer energy from the input voltage to the output voltage. During the ON state of the switch, the input voltage is applied to the inductor causing current to flow through it and energy to be stored in its magnetic field. At the same time, the capacitor is charged to the same voltage as the input voltage. During the off-state switch, the inductor releases the stored energy to the capacitor and load, delivering power to the output. The capacitor supplies energy to the load during the next ON state of the switch. By carefully controlling the switch on-time and off-time, zeta converters can achieve high voltage gains and efficient power transfer. The advantage of zeta converters is that they can be used in a variety of applications, such as those requiring high input voltages and low output voltages, or vice versa. It can

also be used to provide a regulated output voltage even when the input voltage is variable. However, zeta converters have some challenges. The need for careful design to ensure stability and avoid voltage spikes. Additionally, the high-frequency switching used in zeta converters can generate electromagnetic interference, which can cause problems in sensitive electronics. These challenges can be addressed through careful circuit design and component selection, and use of appropriate components. ZETA Converter It consists of a single MOSFET switch, inductors L1 and L2, intermediate capacitor C1, output capacitor C2, and load resistor R. Coupled inductors can be used to minimize board space. Fig.1.4 depicts the zeta converter's topology's circuit configuration.

ZETA converters have no right-half plane null and can be more easily compensated for wider loop bandwidth and better load transient results with smaller output capacitance values. A converter topology provides a positive output voltage from an input voltage that varies above or below the output voltage. A ZETA converter also requires two inductors and a series capacitor, sometimes called a flying capacitor. A ZETA converter consists of a buck controller driving a high-side P-channel MOSFET. ZETA converters are another option for regulating unregulated input power sources like cheap wall warts. An application for the ZETA converter is the charging of automotive batteries from SMPS and solar cells. A Zeta converter is a fourth-order DC-DC converter made up of two inductors and two capacitors and capable of operating in either step-up or step-down mode. Compared with other converters in the same class, such as Cuk and SEPIC converters, the Zeta converter has received the least attention, and more importantly, its dynamic modelling and control have never been reported before in the literature. It presents dynamic modelling and control of a Zeta converter operating in Continuous Conduction Mode (CCM). The State-Space Averaging (SSA) technique is applied to find small-signal linear dynamic model of the converter and its various transfer functions. Based on the derived control-to-output transfer function, the PWM feedback controller is designed

to regulate the output voltage. Results show that the converter exhibits good performance in steady state and during a step-load change.

The ZETA converter provides a positive output voltage for input voltage that varies above and below the output voltage. The ZETA converter also needs two inductors and a series capacitor, sometimes called a flying capacitor. The zeta converter is used for to give the gate pulse for MOSFET which is used the driver circuit in our paper we can see that how the gate pulse is given to it, this converter which is configured with a standard boost converter, the ZETA converter is configured from a buck controller that drives a high-side PMOSFET. The ZETA converter is another option regulating an unregulated input-power supply. All non conventional system energy system require particular power converters. seen the power electronic converter is the of the entire system, show proper design necessary. ZETA Converter Is mentioned and it is use provide positive output from the input voltage it can be used to increase as well as decrease the voltage. This converter is used for power factor correction applications and short circuit protection

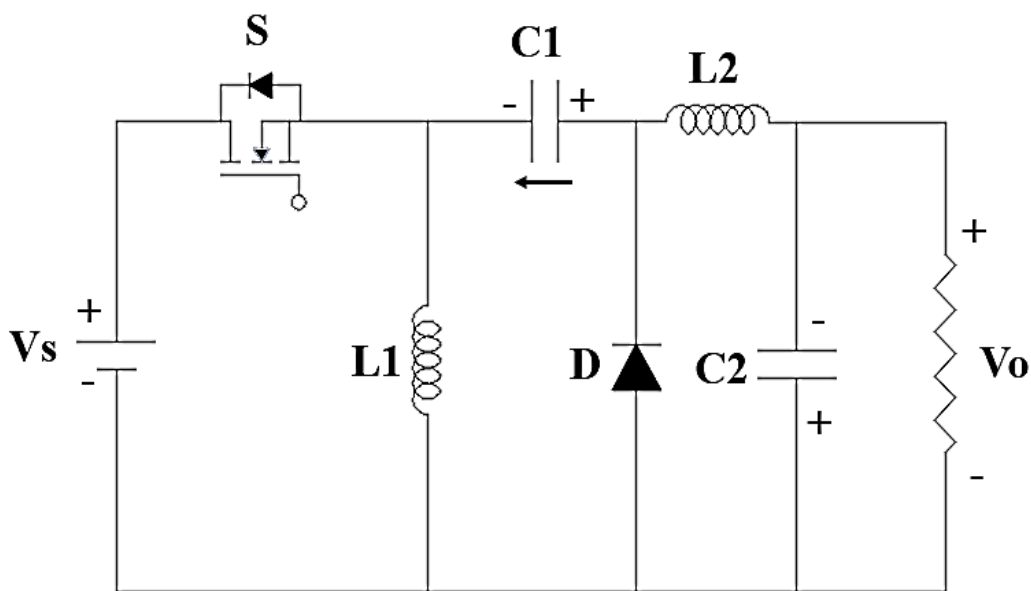


Fig. 1.4 Zeta Converter's Circuit Diagram

1.5 CUK CONVERTER

A Cuk converter is used to increase or decrease DC output voltage. It is a type of DC-DC converter and it is a cascade of a buck converter and a boost converter via

a series capacitor. This capacitor is the main storage element that transfers energy from the input side to the output side compared to traditional DC-DC converters that use inductors as storage elements. In the non-isolated Cuk converter, the input and output circuits share the common ground. The non-isolated Cuk converter topology consists of DC input voltage source V_{in} , input inductor L1, one controllable switch S, energy transfer capacitor C1, diode D, filter inductor L2, filter capacitor C2, and load resistance R. This converter exchanges energy between the inductor L1, capacitor C1, and inductor L2 to convert input DC voltage to required output voltage level. A power transistor switch (S1) such as a MOSFET is used to control the amount of energy exchanged. Fig.1.5 depicts the Cuk converter's topology's circuit configuration.

Cuk converters are used in electric vehicle battery management systems, renewable energy integration including input-side solar panels and photovoltaic applications to facilitate regulation and maximum power point (MPP) operation, and high voltage applications. is ideal for use negative output voltage and low standby current. In hybrid solar-wind energy systems, a Cuk converter is used as a regulator to maintain a constant output voltage where the input voltage is affected by the speed of the sun and wind. The voltage regulation for the DC application systems uses a Cuk converter. The Cuk converter consists of single MOSFET switch, inductors L1 and L2, intermediate storage capacitor C1, output capacitor, C2 and load resistor R. Based on the interconnection of several buck and boost converters in cascade or cascade form, variants like Cuk, SEPIC, and Zeta converters are derived. A Cuk converter, also known as optimum topology converter, is essentially a boost converter followed by a buck converter, but they share the same switching device. It is key to note that the output capacitor of the boost converter functions as the energy source for the buck converter. The Cuk converter can be incorporated to yield either voltage step-up or step-down, thus making it a top choice for a wide range of voltage requirements. Also, it uses a capacitor as the key energy storage component whereas most of the other power converters employ inductors for that purpose. The converter design is such that the current flowing through the input side is always continuous irrespective of the

state of the switch. This also aids in achieving a very low output voltage ripple as a second-order low pass filter is formed by the combination of inductors and capacitors. In addition, the design of inductors ensures zero-ripple behaviour. Since the currents are non-pulsating, electromagnetic interference (EMI) can be significantly reduced by incorporating this topology. Thus, it also leads to inherently lower noise and higher overall efficiency. The topology of a Cuk converter involves a low-side switch, diode, inductors, and a coupling capacitor between the input and output terminals. In the conventional topology, the inductors are typically uncoupled. Few variants of the basic topology incorporate coupled inductors instead that are typically matched in value. In some other cases, the coupled inductors are integrated with a transformer that additionally offers enhanced step-up, volume reduction, and isolation features.

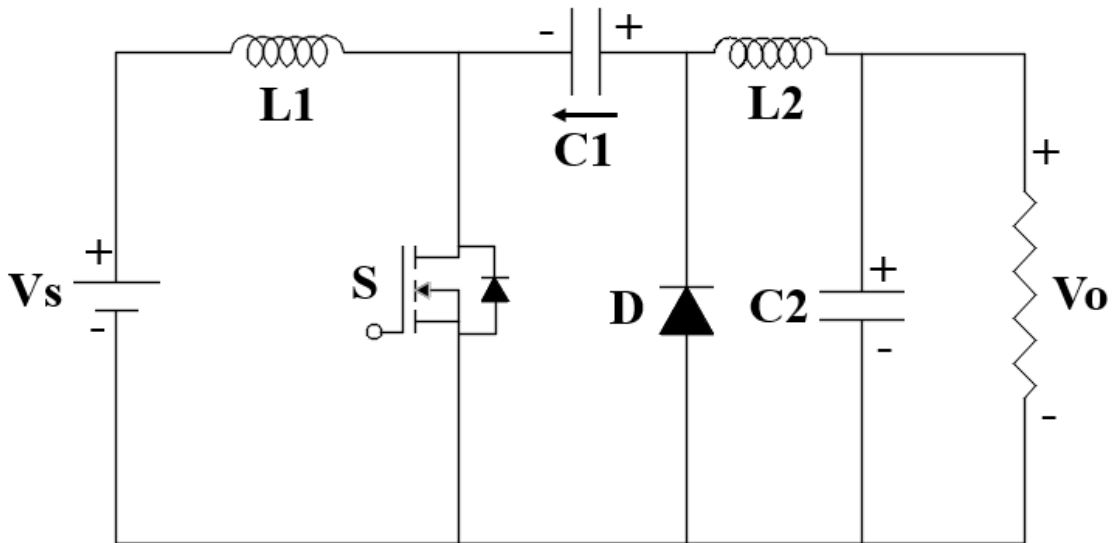


Fig.1.5 Cuk Converter's Circuit Diagram

1.6 QUASI Z-SOURCE CONVERTER

A quasi-Z-source converter is a type of power electronics circuit that provides voltage boosting and inverting capabilities with improved reliability and efficiency. It uses an impedance network to couple the input and output sides of the converter and can operate in both continuous and discontinuous conduction

modes. The quasi-Z-source converter has several advantages over traditional power converters, including the ability to handle a wider range of input voltages and the ability to handle short-circuit faults without damage. It is commonly used in renewable energy systems, electric vehicles, and other applications where efficient power conversion is required. The quasi-Z-source converter uses a unique impedance network, called a quasi-Z-source network, to provide a high degree of input-output isolation and voltage conversion. One of the key advantages is the ability to handle a wider range of input voltages, which can be particularly useful in renewable energy systems that may experience large variations in input voltage.

Another advantage of the converter is the ability to handle short-circuit faults without damage. This is because the impedance network limits the current that can flow through the converter, preventing damage to the circuit. The converter can be used in a variety of applications, including renewable energy systems, electric vehicles, and motor drives. It is particularly well-suited for applications that require a high degree of reliability and The efficiency of the converter can be as high as 98%, depending on the specific configuration and operating conditions. This makes it a highly efficient choice for power conversion applications. One of the challenges of the quasi-Z-source converter is the complexity of the circuit. The impedance network requires precise tuning to achieve optimal performance, and the circuit can be difficult to design and implement. However, several design tools and simulation software packages are available to help simplify the design process. The Quasi Z-source converter is compact, less expensive, and has a high efficiency. It is used in wide range for high power with medium voltage applications. It consists of two MOSFET switches, inductors L1 and L2, diodes D1 and D2, intermediate storage capacitor C1, C2, C3 and C4 and load resistor R. Fig. 1.6 depicts the circuit setup for the Quasi Z-source converter topology. Quasi-Z-source dc-dc converter has a unique LC impedance network that can output positive polar boost voltage and negative polar buck-boost voltage. Quasi-Z-source dc-dc converter has continuous input current, low voltage stress on capacitors, and sharing the input and output grounds.

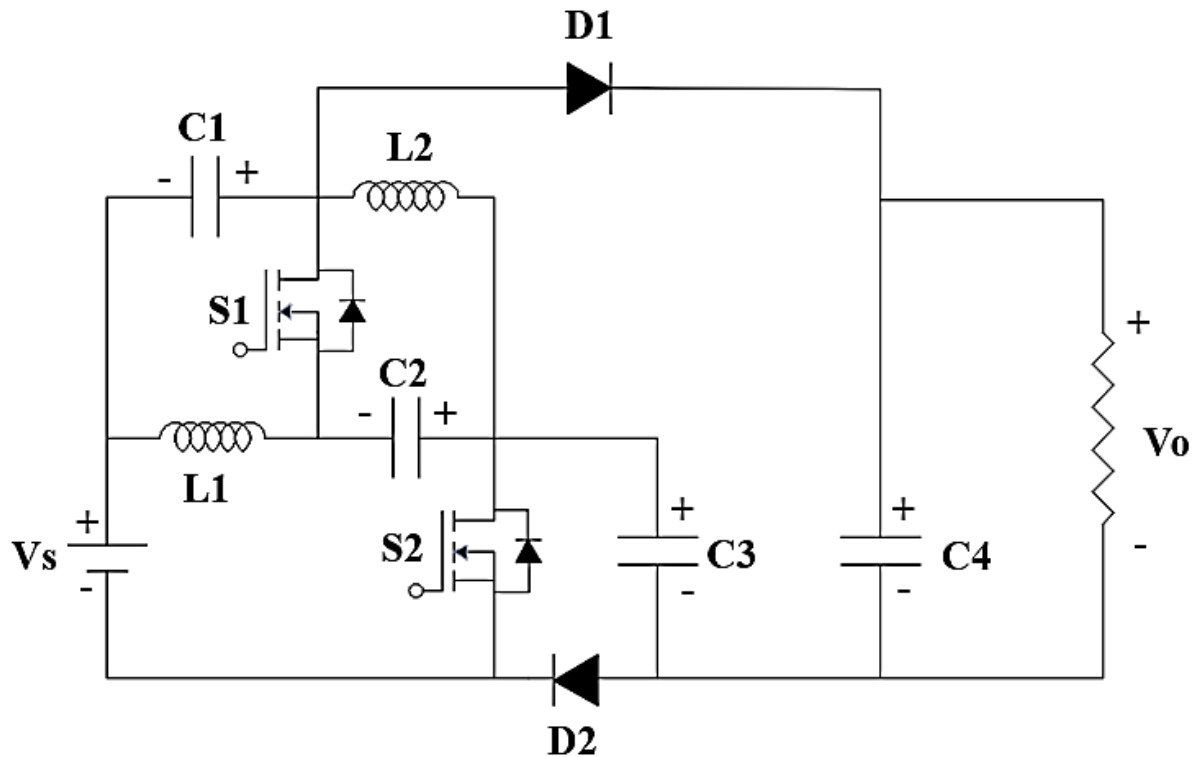


Fig. 1.6 Quasi-Z Source Converter's Circuit Diagram

1.8 OBJECTIVE OF THE PROJECT

The main objective of this project is to design and develop modified SEPIC converter which is suitable for BLDC based system with increased potential and high power rating of applications. It has better efficiency, minimal ripple output, low harmonic distortion and high current and voltage.

1.9 ORGANISATION OF THE REPORT

The organization of the report gives the overview of all the chapters discussed in this report.

CHAPTER 1: The proposed System various converter topology, existing system and Objective of this project are discussed.

CHAPTER 2: Literature survey of this project is described.

CHAPTER 3: Describes about design consideration of the Modified SEPIC, Zeta, Cuk, Quasi-z source converters.

CHAPTER 4: Describes the simulations output waveforms and comparison between the proposed converter and various converters.

CHAPTER 5: Describes the hardware components for the proposed converter.

CHAPTER 6: Describes the conclusion and future scope.

CHAPTER 2

LITERATURE SURVEY

CHAPTER 2

LITERATURE SURVEY

2.1 POWER FACTOR CORRECTION IN CUK-SEPIC-BASED DUAL-OUTPUT-CONVERTER-FED SRM DRIVE

Publication: IEEE Trans. Industrial Electronics, vol. 65, no. 2, pp. 1117-1127, Feb. 2018.

Authors: Anand and B.Singh.

In this paper, a power factor correction (PFC)-based switched reluctance motor (SRM) drive is proposed. Generally, the SRM drive is fed with a simple diode bridge rectifier followed by a bulky capacitor, which draws peaky current at low power factor and high-input-current total harmonic distortion (THD). Here, a dual output converter is proposed to control the SRM and to provide power quality improvement as well. This converter is a combination of Cuk and SEPIC converters, which produces two equal output voltages with neutral point N, to feed a midpoint converter of the SRM drive. The converter is designed to operate in discontinuous conduction mode of operation to obtain inherent PFC at supply side. The motor control is attained by regulating dc link voltage over a wide range. Test results on a prototype of the SRM drive demonstrate the excellent performance with high power factor and reduced input current THD.

2.2 POWER FACTOR CORRECTION IN BRIDGELESS-LUO CONVERTER FED BLDC MOTOR DRIVE

Publication: IEEE Transactions of Industry Applications, Vol. 51, No.2, 2015.

Authors: Bhim Singh, Vashit Bist, Chandra A, and Al-Haddad K.

This paper presents a power factor correction (PFC)-based bridgeless Luo (BL-Luo) converter-fed brushless dc (BLDC) motor drive. A single voltage sensor is used for the speed control of the BLDC motor and PFC at ac mains. The voltage follower control is used for a BL-Luo converter operating in discontinuous inductor current mode. The speed of the BLDC motor is controlled by an approach of variable dc-link voltage, which allows a low-frequency switching of the voltage source inverter for the

electronic commutation of the BLDC motor, thus offering reduced switching losses. The proposed BLDC motor drive is designed to operate over a wide range of speed control with an improved power quality at ac mains.

2.3 BRIDGELESS PFC MODIFIED SEPIC RECTIFIER WITH EXTENDED GAIN FOR UNIVERSAL INPUT VOLTAGE APPLICATIONS

Publication: IEEE Transactions of Power Electronics, Vol.30, No.8, 2015.

Authors: Al-Gabri AM, Fardoun AA and Ismail EH.

In this paper, a new single-phase ac-dc PFC bridgeless rectifier with multiplier stage to improve the efficiency at low input voltage and reduce the switch-voltage stress is introduced. The absence of an input rectifier bridge in the proposed rectifier and the presence of only two semiconductor switches in the current flowing path during each switching cycle result in less conduction losses and improved thermal management compared to the conventional full bridge topology. Lower switch voltage stress allows utilizing a MOSFET with lower R_{DS-on}. The proposed topology is designed to operate in discontinuous conduction mode (DCM) to achieve almost a unity power factor and low total harmonic distortion (THD) of the input current. The proposed topology is compared with modified full-bridge SEPIC rectifier in terms of efficiency, THD, and power factor. Detailed converter analysis, small signal model, and closed-loop analysis are presented.

2.4 MODIFIED ISOLATED POWER FACTOR CORRECTION CUK-CONVERTER FED BLDC MOTOR DRIVE WITH FUZZY LOGIC CONTROLLER FOR PUMPING APPLICATIONS

Publication: Journal of the Chinese Institute of Engineers, Vol. 43, July 2020.

Authors: N. Kumarasabapathy, M. Ramasamy

In this paper presents Water pumps are mostly used for supplying water to industries, commercial establishments, houses, hospitals, private residents, city water systems, agricultural irrigation, etc. Water pumping systems operated by three-phase induction motors reduce the Power Factor (PF) of the electrical network. To decrease the effect

of poor PF, Power Factor Correction (PFC) circuits are added to the AC input side of the water pumping system to enhance the efficiency and PF of the system. This paper presents a Fuzzy Logic Controller (FLC) based modified Power Factor Correction Cuk Converter (PFCCC) operated Voltage Source Inverter (VSI) fed Brushless DC (BLDC) motor drive for agricultural water pumping applications. MATLAB/Simulink simulation results and experimental prototype model results are presented to validate the performance of the designed system.

2.5 FUZZY AND PID CONTROLLERS FOR BUCK-BOOST CONVERTER FED BRIDGELESS BLDC MOTOR OVER CLOUD

Publication: International Conference on Intelligent Data Communication Technologies and Internet of Things (ICICI), Jan. 2019.

Author: Dinesh Gopal, Umasankar Periasamy and Mohana Periyasamy

In this paper emerges with smart features from the past ten years regarding to converter. Since buck-boost converter using BLDC motor drive through Source as Voltage source Inverter (VSI) analysed by two difference controllers like FUZZY and PID controller. Converter has application in different fields with roles and many types of research have been done to bring this topology closer to the real-time application. The proposed converter operates well when there is a discontinuity in the inductor current mode, and it uses a one sensor that checks DC control to improve power quality. This paper shows the output in the improvement of bridgeless BLDC based motor drive and the drive performance are presented.

2.6 CONTROL AND ANALYSIS OF BIDIRECTIONAL INTERLEAVED HYBRID CONVERTER WITH COUPLED INDUCTORS FOR ELECTRIC VEHICLE APPLICATIONS

Publication: Springer Publications, Nov. 2019.

Author: Hedra Saleeb, Khairy Sayed, Ahmed Kassem and Ramadan Mostafa.

In this paper proposes a novel bidirectional interleaved hybrid converter which uses coupled inductors (CIs) for battery electric vehicles (BEVs) in order to optimize the

performance of the power train. In this paper, a hybrid converter is proposed and designed to realize the integration of the DC/DC converter, and DC/AC inverter together in the BEVs power train with high performance in any operating mode, acting as a backup generator to supply emergency power directly to home. The proposed hybrid converter can improve the system cost, volume, and increase efficiency and reliability. This integrated magnetic design structure reduces the size and improves the converter performance, both steady state and transient. A detailed study of the operating principle and design considerations is presented.

2.7 INTERLEAVED BIDIRECTIONAL DC - DC CONVERTER FOR ELECTRIC VEHICLE APPLICATIONS BASED ON MULTIPLE ENERGY STORAGE DEVICES

Publication: Springer Publications, May 2020.

Authors: Rodnei Regis de Melo, Fernando Lessa Tofoli, Sergio Daher and Fernando Luiz Marcelo Antunes

This paper proposes a novel bidirectional interleaved hybrid converter which uses coupled inductors (CIs) for battery electric vehicles (BEVs) in order to optimize the performance of the power train. In this paper, a hybrid converter is proposed and designed to realize the integration of the DC/DC converter, and DC/AC inverter together in the BEVs power train with high performance in any operating mode, acting as a backup generator to supply emergency power directly to home. The proposed hybrid converter can improve the system cost, volume, and increase efficiency and reliability. Here, interleaving structure is used to increase power rating, reduce the input current ripple, output voltage ripple, power loss, and increase efficiency. The performance of the converter is improved by using CIs of energy storage inductors. This integrated magnetic design structure reduces the size and improves the converter performance, both steady state and transient. A detailed study of the operating principle and design considerations is presented.

CHAPTER 3

DESIGN CONSIDERATION OF

CONVERTER TOPOLOGIES

CHAPTER 3

DESIGN CONSIDERATION OF CONVERTER TOPOLOGIES

The design considerations and analysis for the investigation of suitable low ripple and high power converters, the following topologies are taken into account: Modified SEPIC, ZETA, cuk, and Quasi Z-source converters.

3.1 DESIGN EQUATION OF MODIFIED SEPIC CONVERTER

The Leakage and Magnetizing Inductance, L1 & L2 can be expressed as,

$$L = \frac{V_s D}{f_s * \Delta I_L} \quad (1)$$

For ΔIL , assuming for design calculation as 4.8% of **ILoad**.

$$L_1 = L_2 = \frac{24 * 0.67}{33.3 * 0.048} = 10 \text{ mH}$$

Where, Vs - Source voltage (v), D - duty cycle, fs - switching frequency (kHz), ΔIL - change in load currents. The Intermediate capacitors, C1 & C4 can be calculated from the following equation.

$$C = \frac{V_o D}{R * f_s * \Delta I_C} \quad (2)$$

For ΔVC , assuming for design calculation as 2% of **V0**.

$$C_1 = C_4 = \frac{48 * 0.67}{1 * 33.3 * 0.96} = 1000 \mu\text{F}$$

Where, Vo - output voltage (v), D - duty cycle, fs - switching frequency (kHz), ΔVC - change in capacitive voltage. The Output filter capacitors, C2 & C3 are large enough to filter the output ripples.

$$C_2 = C_3 = 1200 \mu\text{F} \text{ (Kept as constant)}$$

Component values are derived and used in the Modified SEPIC Simulation.

Table 3.1 Specifications of Modified SEPIC Converter

S.no	Components	Values
1	Leakage Inductor, L1	10 mH
2	Intermediate Capacitor, C1&C4	1000 μ F
3	Magnetizing Inductor, L2	10 mH
4	Output Capacitor, C2 & C3	1200 μ F
5	Switch x 4	MOSFET
6	Resistive Load, R	100 Ω
7	Switching frequency, fs	33 kHz

3.2 DESIGN EQUATION OF ZETA CONVERTER

A straightforward Zeta converter design example is provided in the following section. The converter's input voltage is $V_s = 24v$, and its output must remain at 72v. The load resistance may be between 50 and 100Ω . The duty cycle D can be calculated by,

$$D = \frac{V_o}{V_d + V_o} \quad (3)$$

The inductors L1 and L2 can be obtained from the equation (4) and (5).

$$L_1 \geq \frac{(1-D)^2 * R_o}{2Df_s} \quad (4)$$

$$L_2 \geq \frac{(1-D)*R_o}{2f_s} \quad (5)$$

The sizing of capacitor C1 can be expressed as,

$$C_1 \geq \frac{D*I_o}{\Delta V_{C1}*f_s} \quad (6)$$

Similarly, the sizing of capacitor C2 can be expressed as,

$$C_2 \geq \frac{(1-D)*V_o}{8*\Delta V_{C1}*L_2*f_s^2} \quad (7)$$

Based on the above equations, component values are calculated and used in the simulation of ZETA converter which is presented in Table 3.2.

Table 3.2 Specifications of Zeta Converter

S.no	Components	Values
1	Inductors, L1 & L2	1.6mH
2	Capacitor, C1	150μF
3	Output Capacitor, C2	720μF
4	Resistive Load, R	100Ω
5	Switching frequency, fs	25kHz

3.3 DESIGN EQUATION OF CUK CONVERTER

The average value of input voltage is expressed as,

$$V_{in} = \frac{2\sqrt{2}V_s}{\pi} \quad (8)$$

The duty cycle ratio, D can be given as,

$$\frac{V_o}{V_s} = \frac{D}{1-D} \quad (9)$$

The input inductance, L1 can be determined by,

$$L_1 = \frac{DV_{in}}{\Delta IL_1 f_s} \quad (10)$$

The output inductance, L2 can be determined by,

$$L_2 = \frac{(1-D)DV_{dc}}{\Delta IL_2 f_s} \quad (11)$$

The intermediate capacitor, C1 can be expressed as,

$$C_1 = \frac{DI_{dc}}{\Delta V_{C1} f_s} \quad (12)$$

The output capacitor, C2 can be expressed as,

$$C_2 = \frac{I_{dc}}{\omega * \Delta V_{C2}} \quad (13)$$

Based on the above equations, component values are calculated and used in the simulation of Cuk converter, which is presented in Table 3.3

Table 3.3 Specifications of Cuk Converter

S.no	Component	Value
1	Inductors, L1 & L2	18 mH
2	Capacitor, C1	200 μ F
3	Output Capacitor, C2	720 μ F
4	Resistive Load	100 Ω

3.4 DESIGN EQUATION OF QUASI Z-SOURCE CONVERTER

The input inductor L1 can be determined by,

$$L_1 \geq \frac{D(1-D)V_s}{\Delta i_{L1}f_s(1-2D)} \quad (14)$$

Similarly, inductor L2 can be determined by,

$$L_2 \geq \frac{D(1-D)V_s}{\Delta i_{L2}f_s(1-2D)} \quad (15)$$

The Capacitors C1-4 value can be determined by,

$$C_1 \geq \frac{I_{L2}(1-D)}{\Delta V_{C1}f_s} \quad (16)$$

$$C_2 \geq \frac{I_{L2}(1-D)}{\Delta V_{C2}f_s} \quad (17)$$

$$C_3 \geq \frac{I_o}{\Delta V_{C3}f_s} \quad (18)$$

$$C_4 \geq \frac{I_o(1-D)}{\Delta V_{C4}f_s} \quad (19)$$

Based on the above equations, component values are calculated and used in the simulation of Quasi Z-source converter, which is presented in Table 3.4

Table 3.4 Specifications of Quasi-Z Source Converter

S.no	Components	Values
1	Inductors, L1	20mH
2	Input Filter Capacitor, C1	200 μ F
3	Magnetizing inductor, L2	720 μ F
4	Storage Capacitors, C2 & C3	650 μ F
5	Output Capacitor, C4	1000 μ F
6	Resistive Load, R	100 Ω

CHAPTER 4

SIMULATION AND PERFORMANCE ANALYSIS FOR THE PROPOSED CONVERTER AND THE AFOREMENTIONED CONVERTERS

CHAPTER 4

SIMULATION AND PERFORMANCE ANALYSIS FOR THE PROPOSED CONVERTER AND THE AFOREMENTIONED CONVERTERS

The purpose of comparison, all of the aforementioned converters are powered by 24v Li-ion batteries with a combined maximum current capacity of 110Ah.

4.1 OUTPUT RESPONSE AFOREMENTIONED CONVERTERS

This chapter shows the simulated output response of the various converters, the validation process goes into great detail for the calculations such as input and output voltage, supply current, voltage gain and efficiency.

4.1.1 MODIFIED SEPIC CONVERTER

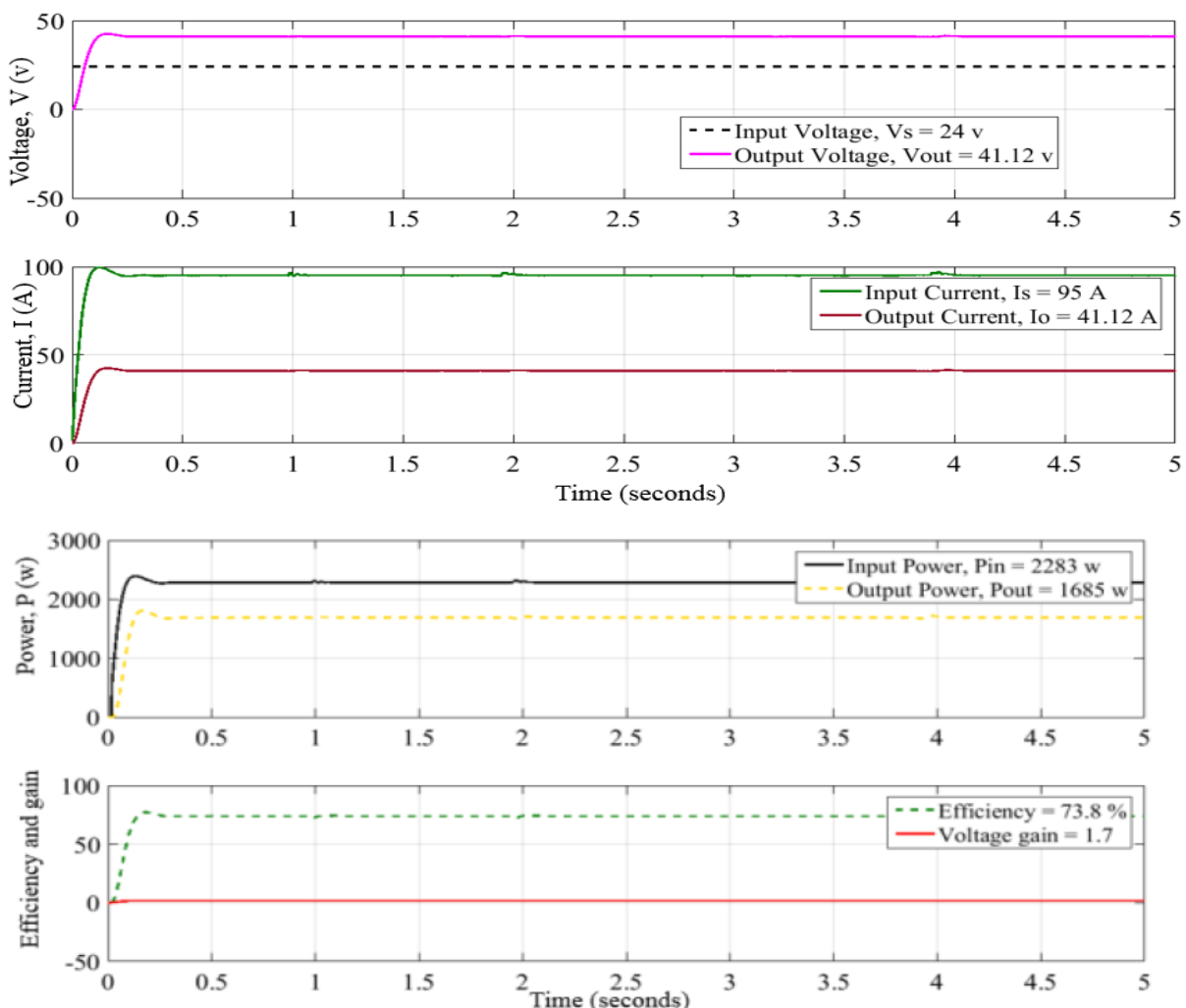


Fig. 4.1 Output Response of Modified SEPIC Converter

The output response of Modified SEPIC is illustrated in Fig. 4.1 The input voltage, V_s , is specified as 24 volts, and the supply current, I_s , is 95A. The converter produced a 41.2v output voltage and a 41.12A output current. It is 1.99 times for the voltage conversion ratio. The converter has an efficiency rate of 73.8%

4.1.2 ZETA CONVERTER

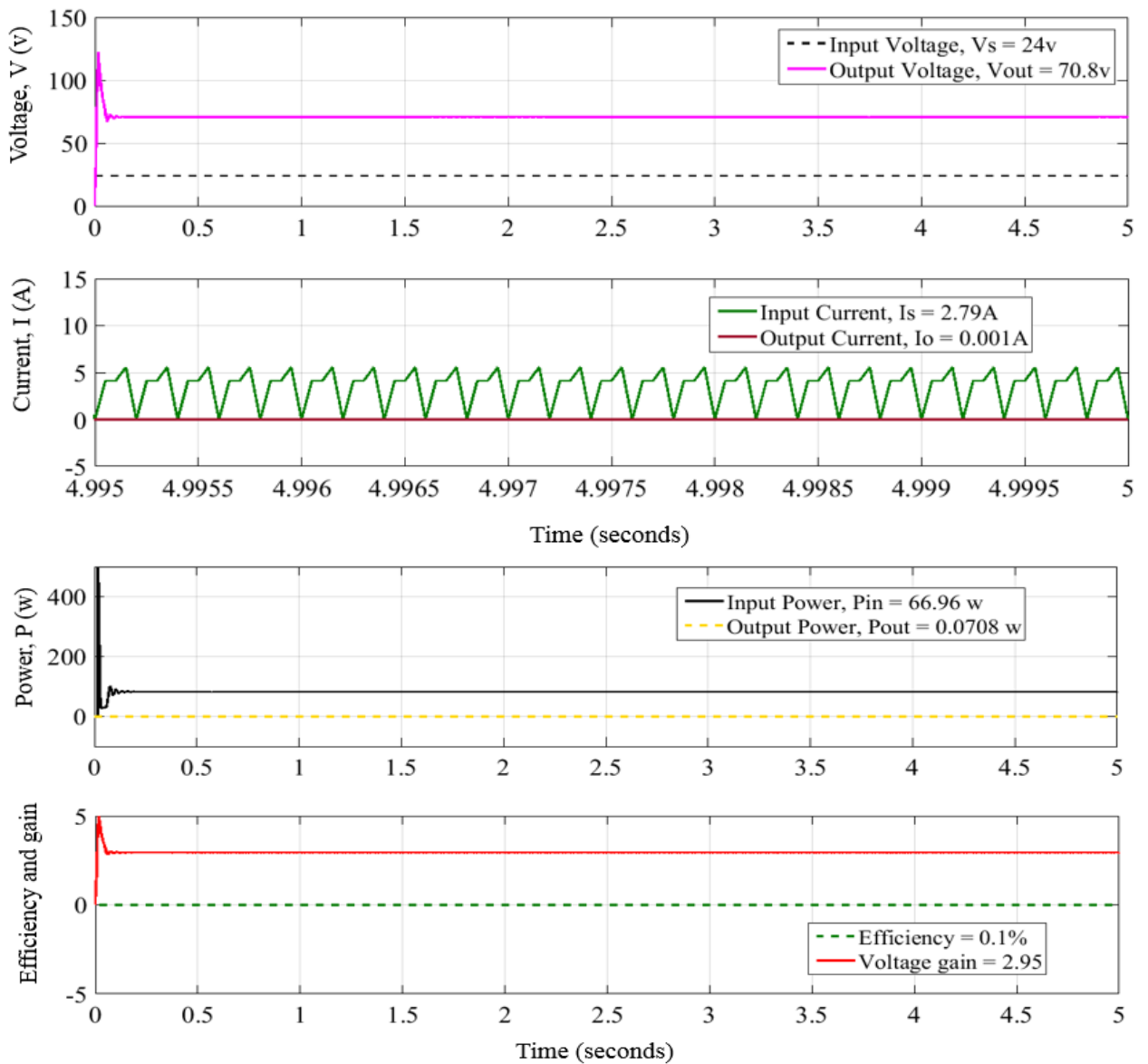


Fig. 4.2 Output Response of Zeta Converter

The output response of ZETA converter is illustrated in Fig. 4.2 The input voltage, V_s , is specified as 24 volts, and the supply current, I_s , is 2.79A. The converter produced a 70.8v output voltage and a 0.001A output current. It is 2.95 times for the voltage conversion ratio. The converter has an efficiency rate of 0.1%.

4.1.3 CUK CONVERTER

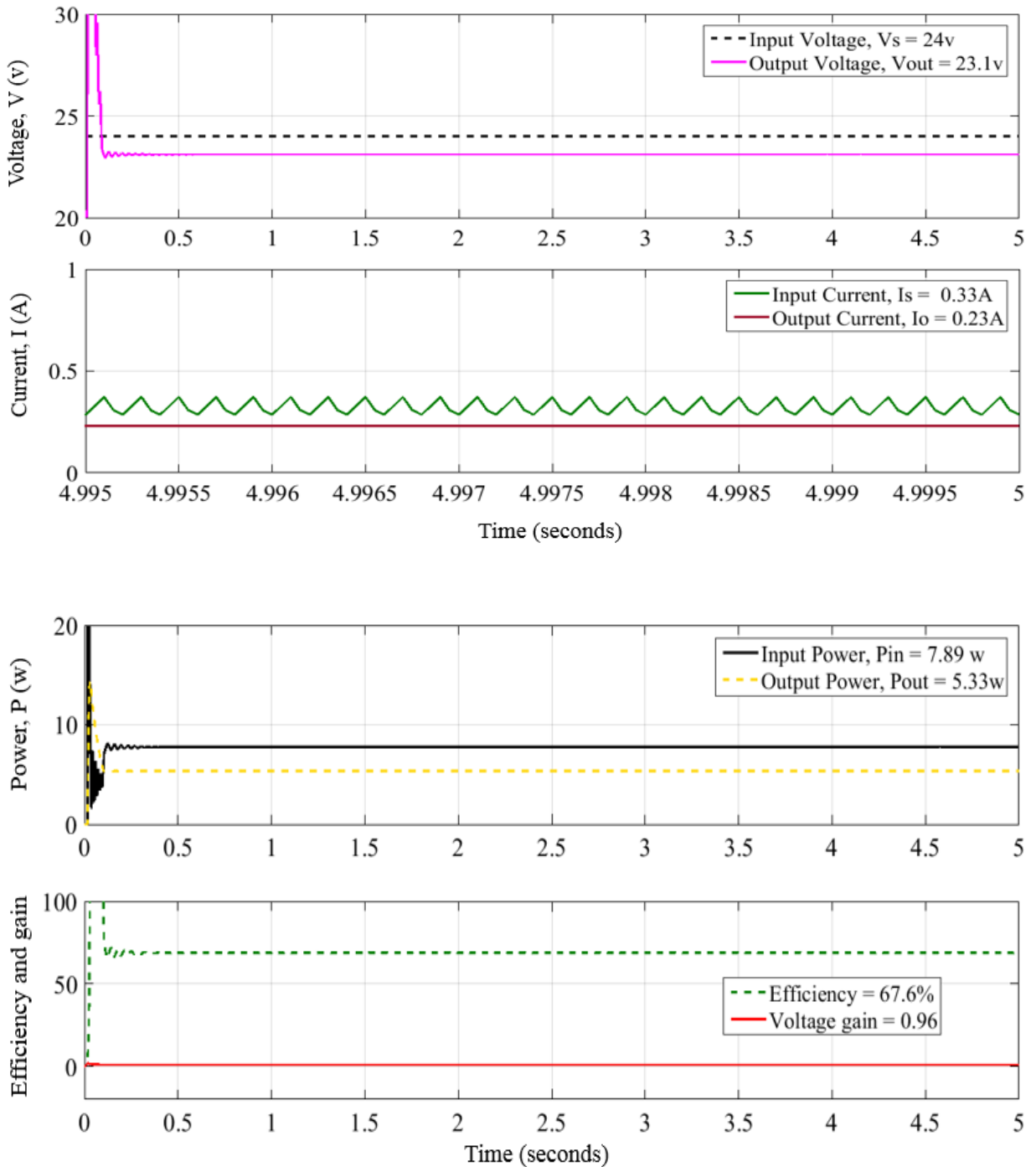


Fig. 4.3 Output Response of Cuk Converter

The output response of cuk converter is illustrated in Fig. 4.3 The input voltage, Vs, is specified as 24 volts, and the supply current, Is, is 0.33 A. The converter produced a 23.1v output voltage and a 0.23A output current. It is 0.96 times for the voltage conversion ratio. The converter has an efficiency rate of 67.6%.

4.1.4 QUASI Z-SOURCE CONVERTER

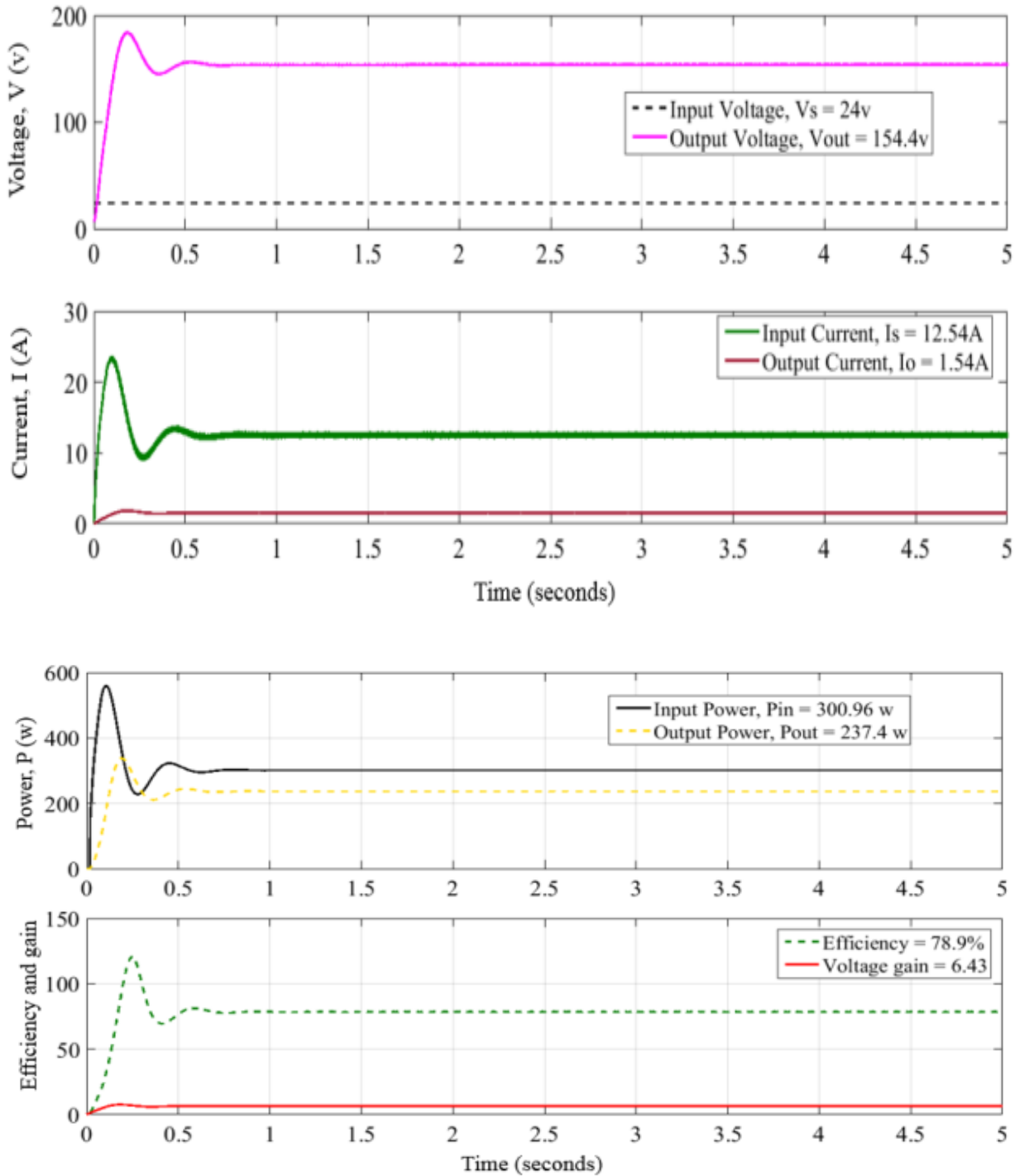


Fig. 4.4 Output Response of Quasi Z-Source Converter

The output response of Quasi Z-source converter is illustrated in Fig. 4.4. The input voltage, V_s , is specified as 24 volts, and the supply current, I_s , is 12.54 A. The converter produced a 154.4v output voltage and a 1.54A output current. It is 6.43 times for the voltage conversion ratio. The converter has an efficiency rate of 78.9%.

4.2 COMPARISON RESULTS BETWEEN THE PROPOSED CONVERTER AND VARIOUS CONVERTERS

In the next part, the output response is analysed to determine a suitable converter that has the lowest output ripple and enough current to power an electric vehicle with a 2 kW BLDC motor. The analysis begins with the output voltage obtained from a 24volt battery supply. Following the analysis of voltage gain values, consider input current ripple. Based on Table 4.2 Comparative Analysis on Efficiency and Voltage Gain, The output load current is directly proportional to the amplitude of the input ripple voltage. At maximum output load, the input ripple amplitude reaches its maximum value. Additionally, the duty cycle of the converter affects the amplitude of the voltage ripple. Based on Table 4.1 Comparative Analysis between the Converter Topologies.

Additional capacitors and inductors can be added to suppress the input current ripple without significantly increasing the current load and losses. However, changing the remaining component values present in the converter topology aims at reducing the current ripple. The input current ripple analysis is shown in Fig. 4.5 and the output voltage waveform is shown in Fig. 4.6 In DC circuits, output voltage ripple wastes energy and has a variety of adverse effects, including component heating, noise and distortion, and possible malfunction of digital circuits. Both voltage regulators and electronic filters can filter out ripple, and this is shown in Fig. 4.7 Large ripple currents can cause many problems.

For example, A switching power supply is a type of electronic power supply that uses a switching regulator to convert electrical power efficiently. It operates by rapidly switching the input voltage on and off, and using a transformer to step down the voltage to the desired level. This process generates high-frequency currents, which can cause problems if they are not properly managed. One issue that can arise is excessive ripple current. Ripple current is the fluctuating current that flows through a circuit as a result of the switching action. This current can cause problems for both the power supply and the load. If the ripple current exceeds approximately 5% of the DC

output current, the power supply may interpret this as a fault condition and trigger the overcurrent safety circuit. This can cause the power supply to shut down, which can be problematic in some applications. Another issue that can arise is instability in the control loop. The control loop of a switching power supply is designed to maintain a stable output voltage or current, but if the load generates ripple currents that are harmonically related to the switching frequency of the power supply, the control loop can become unstable. This can cause the output voltage or current to fluctuate excessively, which can cause problems for the load. In addition to these issues, large ripple currents can overload the switching power supply outputs and accelerate failures. This is because the high-frequency currents generate heat in the components, which can cause them to degrade or fail over time. To prevent these issues, it is important to design the power supply and load to minimize ripple currents, and to use appropriate filtering and protection circuitry to manage them.

4.3 OUTPUT VOLTAGE OBTAINED FROM DIFFERENT CONVERTER TOPOLOGIES

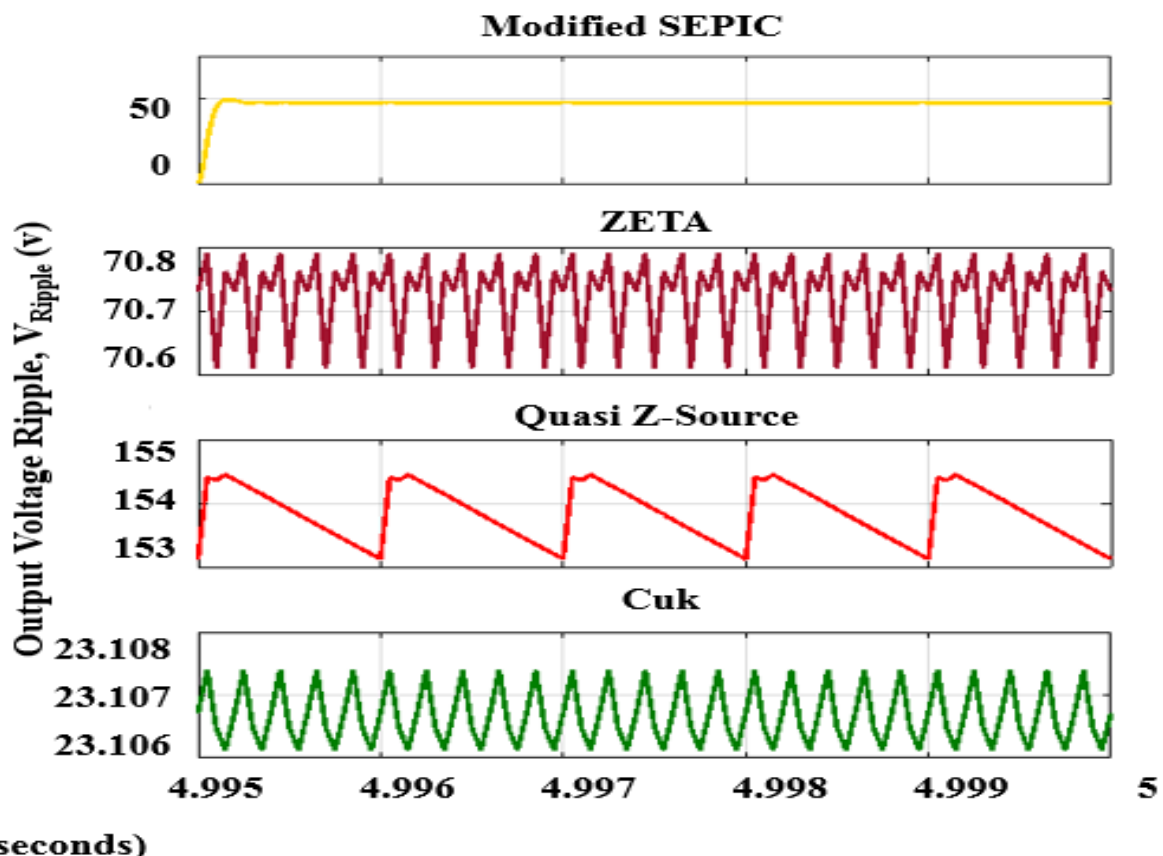


Fig. 4.5 Output Voltage Ripple Analysis

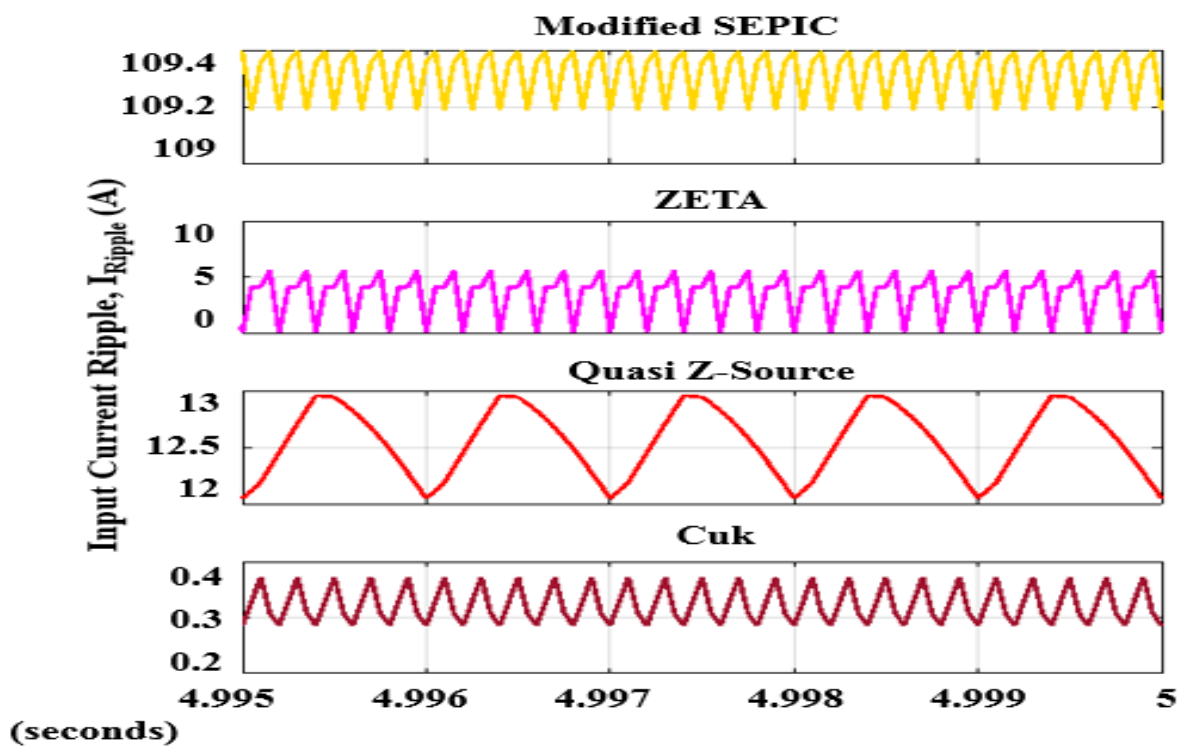


Fig.4.6 Input Current Ripple Analysis

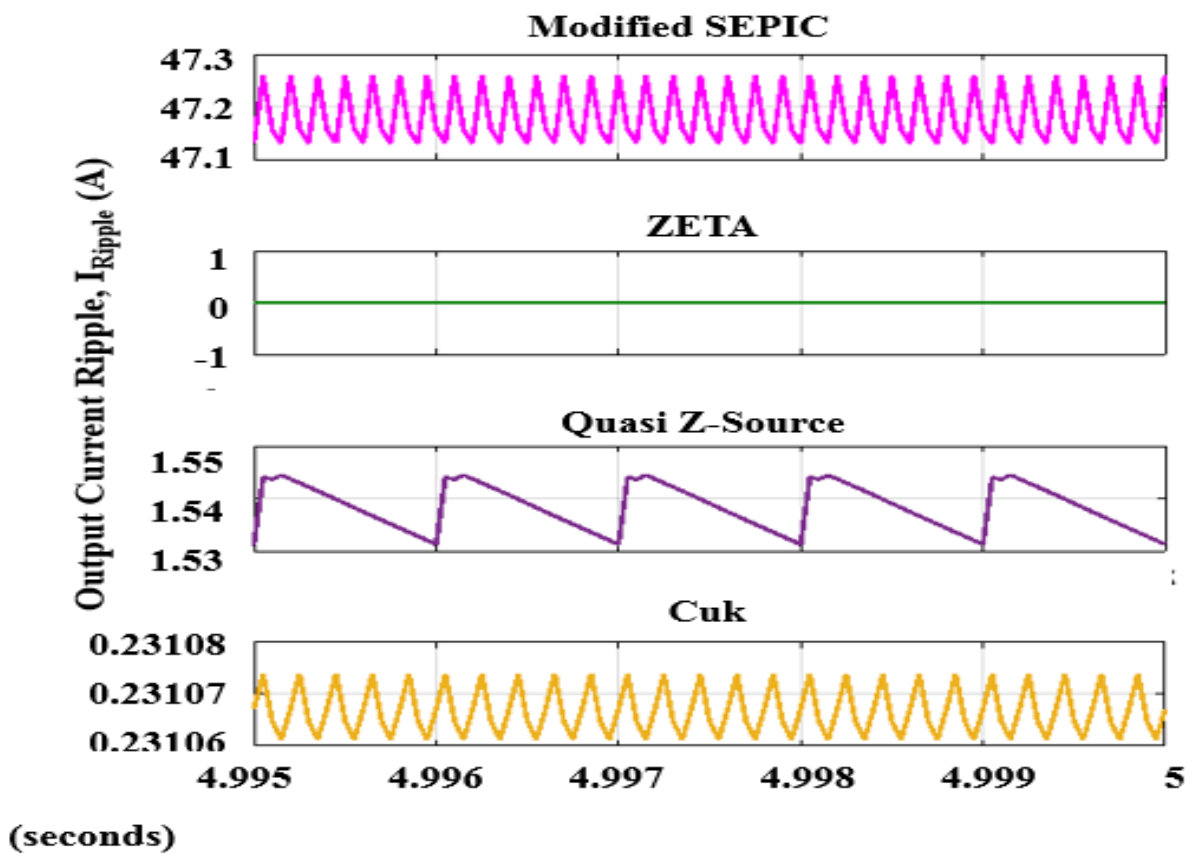


Fig. 4.7 Output Current Ripple Analysis

Table 4.1 Comparative Analysis between the Converter Topologies

Converter Topologies	Input Current, A	Output Voltage, V	Output Current, A	Reduced Output Ripple%	No. of Components
Modified SEPIC	95	41.12	41.12	0.30	11
ZETA	2.79	70.8	0.001	0.40	6
Cuk	0.33	23.1	0.23	0.34	6
Quasi Z-source	12.54	154.4	1.54	0.42	10

Table 4.2 Comparative Analysis on Efficiency and Voltage Gain

Converter Topologies	Pin, W	Pout, W	η , %	n
Modified SEPIC	2283	1685	73.8	1.7
ZETA	66.96	0.0708	0.1	2.95
Cuk	7.89	5.33	67.6	0.96
Quasi Z-source	300.96	237.4	78.9	6.43

CHAPTER 5

EXPERIMENTAL ANALYSIS

CHAPTER 5

EXPERIMENTAL ANALYSIS

5.1 PROTOTYPE PARAMETER

In order to verify the theoretical analysis of the Modified SEPIC converter, a 100W prototype is used and the components used in the prototype are

1. Inductor
2. Capacitor
3. MOSFET switch
4. Diode
5. PIC Microcontroller
6. Gate drive IC

5.1.1 INDUCTOR



Fig 5.1 Coupled Inductor

Inductors are widely used in power electronics converters to regulate voltage and current. The inductor is typically used in combination with other passive and active components, such as capacitors and switches, to form a power converter circuit. In a power converter, the inductor stores energy from the input voltage during the on-time of a switching device (e.g., transistor), and releases the energy to the output during the off-time of the switching device. This action smooths the output voltage and current, reducing ripple and noise. The inductor is an essential component in switching

regulators, which are widely used in power electronics to regulate voltage and current. In a buck converter, for example, the inductor is placed in series with the load and the switching transistor. During the on-time of the transistor, current flows through the inductor, storing energy in the magnetic field. During the off-time, the inductor releases the stored energy to the output, providing a steady output voltage. Similarly, in a boost converter, the inductor is placed in series with the input voltage and the switching transistor. During the on-time of the transistor, current flows through the inductor, storing energy in the magnetic field. During the off-time, the inductor releases the stored energy to the output, providing a higher output voltage than the input voltage. Inductors are also used in other types of converters, such as flyback converters, forward converters, and push-pull converters. The inductor's value and characteristics are critical to the converter's performance, and it is often necessary to choose an appropriate inductor based on the converter's specifications and requirements. The inductors used in Fig.5.1 are input inductor and magnetizing inductor. The core type of the input inductor and the CL is iron powder toroidal core T184-52 and ferrite core EE42/42/15 with 0.3 mm air gap, respectively.

The iron core is used in the area of low space inductors as it have high inductance value with limited high frequency capacity. The ferrite core is used to exhibit the magnetic properties. The initial permeability's are below 100 only. Thus these inductors posses with high temperature co-efficient. The Magnetizing inductance is associated with the flux that actually links the core of the transformer (as opposed to leakage flux, which does not). Leakage inductance derives from the electrical property of an imperfectly-coupled transformer whereby each winding behaves as a self-inductance in series with the winding's respective ohmic resistance constant.

5.1.2 CAPACITOR

The capacitors in Fig.5.2 are clamped capacitor, filter capacitor and intermediate capacitors. The clamped capacitor is a capacitor of a circuit that fixes either positive

or negative peak excursions of a signal to a defined value by shifting its DC value. The capacitor used to filter out a certain frequency and the give the selective value as the output is called filter capacitor or output capacitor. Some other capacitors used in the circuit to store the energy released from magnetizing or leakage inductor are intermediate capacitors. Capacitors are also commonly used in power electronics converters. In converters, capacitors are used to store and release electrical energy, and to filter out high-frequency noise and ripple in the output voltage or current.

In a typical converter circuit, the capacitor is placed in parallel with the load, and in series with the inductor and the switching device (e.g., transistor). During the on-time of the switching device, the capacitor is charged with energy from the input voltage, and during the off-time, the capacitor discharges, providing a steady output voltage or current.

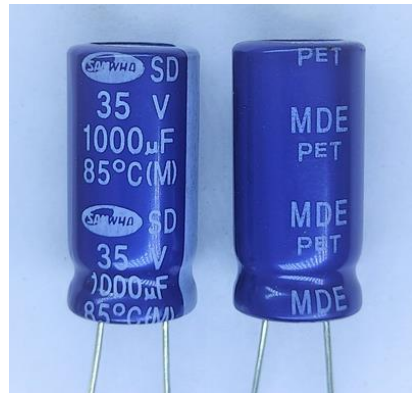


Fig 5.2 Capacitor

The capacitor is often used in combination with the inductor to form a low-pass filter that removes high-frequency noise and ripple from the output. The filter action is based on the fact that the inductor resists change in current, and the capacitor resists changes in voltage. Together, the inductor and capacitor can smooth out the output voltage or current, reducing ripple and noise. The value and characteristics of the capacitor are important in converter design, as they can affect the converter's performance and stability. The capacitance value and the type of capacitor (e.g., ceramic, electrolytic, tantalum) are chosen based on the converter's requirements and specifications. Capacitors are used in various types of converters, including buck converters, boost converters, and flyback converters, among others. The specific

capacitor configuration and placement depend on the converter topology and the design requirements.

5.1.3 MOSFET GATE DRIVER

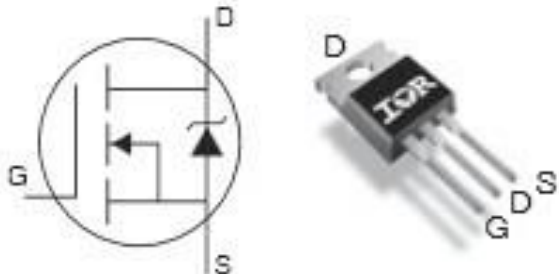


Fig. 5.3 MOSFET

The IRF840B is a power MOSFET transistor designed for high-power applications. Fig.5.3 It is widely used in switching power supplies, motor control. It is an N-channel MOSFET, which means that it is designed to handle negative voltages on its gate. The maximum drain-source voltage (V_{ds}) is 500 volts, which makes it suitable for high-voltage applications. maximum drain current (I_d) is 8 amperes, which allows it to handle high power levels. The on-resistance ($R_{ds(on)}$) is specified as 1.3 ohms maximum, which means that it has low resistance when it is fully turned on, allowing it to dissipate less power and operate more efficiently. The gate threshold voltage ($V_{gs(th)}$) is specified as 2 to 4 volts, which means that a voltage of at least 2 to 4 volts must be applied to the gate to turn the MOSFET on. It is important to note that the IRF840B, like all MOSFETs, is a voltage-controlled device, which means that the voltage applied to the gate determines the state of the transistor. Proper gate drive circuitry and protection is required to ensure the reliable and safe operation of the MOSFET in a given application. MOSFETs (metal-oxide-semiconductor field-effect transistors) are widely used in power electronics converters as switching devices. MOSFETs are preferred over other types of switching devices, such as BJTs (bipolar junction transistors), because they have low on-resistance, high switching speeds, and low gate drive power requirements. In a typical converter circuit, the MOSFET is used to switch the input voltage on and off to create a pulsed output waveform. The

MOSFET acts as a switch, turning on and off according to the input signal applied to its gate terminal. When the MOSFET is turned on, it allows current to flow through the inductor, storing energy in its magnetic field. When the MOSFET is turned off, the inductor releases the stored energy, providing a steady output voltage or current. MOSFETs are used in various types of converters, such as buck converters, boost converters, and flyback converters, among others. The choice of MOSFET depends on the converter's requirements and specifications, such as the maximum input voltage, output current, and switching frequency. MOSFETs also have specific characteristics that need to be taken into account, such as their gate threshold voltage, on-resistance, and maximum power dissipation. MOSFETs are often used in combination with other passive and active components, such as inductors, capacitors, and diodes, to form a complete converter circuit. The design and implementation of the MOSFET and other components must be carefully optimized to ensure the converter's performance, efficiency, and reliability. Gate driver ICs are essential components in many high-power applications, where they play a crucial role in controlling the switching of power devices. These devices are designed to meet the specific requirements of different power electronic applications, and are available in various voltage and current ratings, as well as with different features and functionalities. Some of the key features of gate driver ICs include High output current capability to drive the gates of power transistors effectively, High-speed switching performance to reduce switching losses and improve system efficiency, Integrated protection features such as under-voltage lockout, over-voltage protection, and over-current protection, which help to prevent damage to the power transistor and the IC itself, Adjustable dead-time control to ensure that both high-side and low-side power devices are not switched on simultaneously, which could cause a short circuit, Fault reporting and status indication, which help to diagnose and troubleshoot problems in the system. They are widely used in various applications, such as motor drives, solar inverters, power supplies, and electric vehicles. In Fig.5.4 FAN7392N is

a half-bridge gate driver IC designed for driving MOSFETs and IGBTs in high-power applications, such as motor drives and power supplies.

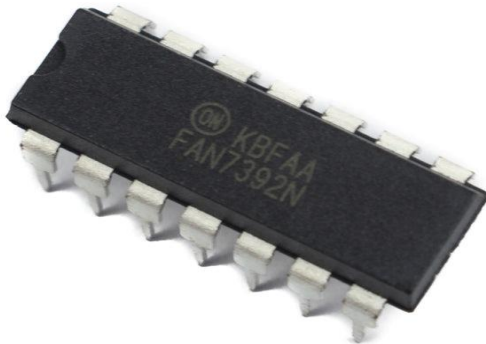


Fig. 5.4 FAN7392N Gate Driver IC

The FAN7392N features a floating high-side driver and a low-side driver that can source and sink up to 1.5A of peak current. It can operate over a wide range of supply voltages, from 10V to 20V, making it suitable for use in various power electronics applications. Some of the key features of the FAN7392N include High output current capability to drive large MOSFETs and IGBTs, Integrated bootstrap diode to provide the necessary voltage to drive the high-side MOSFET gate, Under-voltage lockout and over-current protection features to prevent damage to the device and the power transistors, Integrated dead-time control to ensure that both high-side and low-side MOSFETs are not turned on simultaneously, preventing short circuits, Thermal shutdown protection to prevent the device from overheating. The FAN7392N is available in an 8-pin SOIC package and is rated for operation over a wide temperature range, from -40°C to 125°C. It is widely used in motor drives, power supplies, and other high-power applications, where it helps to improve system efficiency and reliability. The FAN7392N is compatible with both CMOS and TTL input signals, making it easy to integrate into different control circuits. The device has an internal dead-time control circuitry that provides a fixed delay of 260ns between the turn-off of the low-side driver and the turn-on of the high-side driver. This feature helps to prevent shoot-through current and protect the power devices. The FAN7392N has various protection features, such as under-voltage lockout, over-current protection,

and thermal shutdown. These features help to prevent the device from damage due to fault conditions, Wide Operating Range from 10V to 20V. This feature makes it suitable for use in various power electronics applications, The FAN7392N is a cost-effective solution for driving MOSFETs and IGBTs. It eliminates the need for additional external components, such as gate resistors and diodes, which can save both cost and space on the PCB. Gate driver ICs (integrated circuits) are commonly used in power electronics converters to drive high-side and low-side switching devices, such as MOSFETs and IGBTs (insulated-gate bipolar transistors).

Gate driver ICs provide the necessary voltage and current levels to turn on and off the switching devices quickly and reliably, which is essential for converter performance and efficiency. In a typical converter circuit, the gate driver IC is connected to the microcontroller or control circuit and the switching device. The gate driver IC receives a control signal from the microcontroller and amplifies it to provide the necessary voltage and current levels to turn on and off the switching device. The gate driver IC also provides protection features, such as overvoltage and overcurrent protection, to ensure the safe and reliable operation of the converter. Gate driver ICs are available in various configurations, such as single-channel, dual-channel, and multi-channel, to accommodate different converter topologies and switching device configurations. The choice of gate driver IC depends on the converter's requirements and specifications, such as the maximum input voltage, output current, and switching frequency. The design and implementation of the gate driver IC and other components must be carefully optimized to ensure the converter's performance, efficiency, and reliability. Proper circuit layout, shielding, and grounding practices must also be followed to minimize noise and interference in the gate driver IC's operation.

5.1.4 DIODE

Diodes play an important role in DC-DC converters, which are electronic circuits that convert one DC voltage level to another. DC-DC converters can be used in a variety of applications, such as power supplies for electronic devices, battery chargers, and renewable energy systems. One of the most common types of DC-DC

converters is the Buck converter, which is used to step down a DC voltage. When the switch is closed, current flows through the inductor and energy is stored in its magnetic field. When the switch is opened, the diode conducts and allows the energy stored in the inductor to be transferred to the output capacitor, which provides a stable output voltage. During the step-up mode, when the output voltage is greater than the input voltage, the switch is turned on, and current flows through the inductor, storing energy. At this time, the diode is reverse-biased, and it blocks the flow of current from the inductor to the output capacitor.



Fig. 5.5 Diode

During the step-down mode, when the output voltage is lower than the input voltage, the switch is turned off, and the energy stored in the inductor is released through the diode. The diode is forward-biased, and it conducts the current from the inductor to the output capacitor, reducing the voltage across the load. Thus, the diode in the SEPIC converter allows the energy to flow from the input to the output during the step-down mode and prevents the reverse flow of energy during the step-up mode. It is an important component that ensures the proper functioning of the SEPIC converter. The diode in the Buck converter serves as a path for the inductor's energy to flow to the output capacitor when the switch is open. It also serves to block reverse current flow from the output capacitor to the input voltage source when the switch is closed.

In addition to the Buck converter, diodes are also used in other types of DC-DC converters, such as Boost converters, Buck-Boost converters, and SEPIC converters. In each case, the diode serves to control the flow of current through the circuit and ensure proper voltage conversion. Diodes are essential components in power electronics converters, as they are used to control the flow of current and

voltage. In converters, diodes are used in conjunction with other passive and active components, such as capacitors, inductors, and MOSFETs, to create switching circuits that regulate voltage and current. In a typical converter circuit, the diode is placed in parallel with the load and in series with the switching device (e.g., MOSFET). During the on-time of the MOSFET, the diode is reverse-biased and blocks the flow of current. During the off-time of the MOSFET, the diode conducts and allows the inductor to discharge, providing a steady output voltage or current. Diodes are used in various types of converters, such as buck converters, boost converters, and flyback converters, among others. The choice of diode depends on the converter's requirements and specifications, such as the maximum input voltage, output current, and switching frequency. Diodes also have specific characteristics that need to be taken into account, such as their forward voltage drop and reverse recovery time. Fig.5.5 Diodes can also be used in parallel with MOSFETs to form a synchronous rectifier circuit. In this configuration, the diode is replaced with another MOSFET, which is turned on during the off-time of the main MOSFET. This configuration reduces power loss and increases the converter's efficiency. The design and implementation of the diode and other components must be carefully optimized to ensure the converter's performance, efficiency, and reliability.

5.1.5 PIC Microcontroller



Fig. 5.6 16F877A Microcontroller

The PIC16F877A Microcontroller can be used in a variety of power electronics applications, particularly those that require control of power electronic devices such as thyristors, MOSFETs, or IGBTs. Here are a few examples of how the PIC 16F877A can be used in power electronics like Inverters are widely used in renewable energy systems to convert DC power from sources such as solar panels or batteries into AC

power for use in homes or businesses. The PIC 16F877A can be used to control the switching of power electronic devices in the inverter, ensuring efficient and stable operation. In Motor Control PIC 16F877A can be used to control the speed and direction of motors in a variety of applications such as fans, pumps, and conveyor systems. The microcontroller can be used to generate PWM signals to control the speed of the motor, and to monitor feedback signals such as current or voltage to ensure safe and efficient operation. Applications of the PIC 16F877A in Fig.5.6 include industrial control, automotive systems, medical equipment, and consumer electronics. It is also widely used in educational settings to teach embedded systems programming and design. Overall, the PIC 16F877A can be a useful tool in designing and implementing power electronics systems, providing a flexible and cost-effective solution for controlling power electronic devices and monitoring system performance. PIC microcontrollers are commonly used in power electronics converters for control and monitoring purposes.

PIC microcontrollers are small, low-power devices that can interface with other components in the converter circuit and perform control and monitoring tasks, such as regulation, switching, protection, and communication. In a typical converter circuit, the PIC microcontroller is used to generate control signals that drive the switching devices (e.g., MOSFETs) and regulate the output voltage or current. The microcontroller can also monitor various parameters of the converter, such as input voltage and current, output voltage and current, temperature, and fault conditions. PIC microcontrollers are programmed using a high-level language such as C, which allows for rapid development and testing of control algorithms. The microcontroller can also interface with other devices, such as sensors, displays, and communication modules, to provide a complete control and monitoring system for the converter. PIC microcontrollers are used in various types of converters, such as buck converters, boost converters, and flyback converters, among others. The choice of microcontroller depends on the converter's requirements and specifications, such as the control algorithm, communication protocol, and processing power. The design and

implementation of the microcontroller and other components must be carefully optimized to ensure the converter's performance, efficiency, and reliability. Proper circuit layout, shielding, and grounding practices must also be followed to minimize noise and interference in the microcontroller's operation.

CHAPTER 6

CONCLUSION AND FUTURE SCOPE

CHAPTER 6

CONCLUSION AND FUTURE SCOPE

6.1 CONCLUSION

Modified SEPIC Converter is designed & developed and is compared with various converters like Zeta, Cuk and Quasi-Z source converters. With consideration, analysis and output waveforms it is observed that Modified SEPIC converter has high efficiency, low ripple current and voltage, minimal voltage gain, reduced in switching losses. Modified SEPIC converter produces output voltage and output current as 41.2v and 41.12A respectively, it is 1.99 times of the voltage conversion ratio, output ripple is observed as 0.30% with an efficiency of 73.8%. Thus Modified SEPIC converter is suggested for BLDC drive and high power applications.

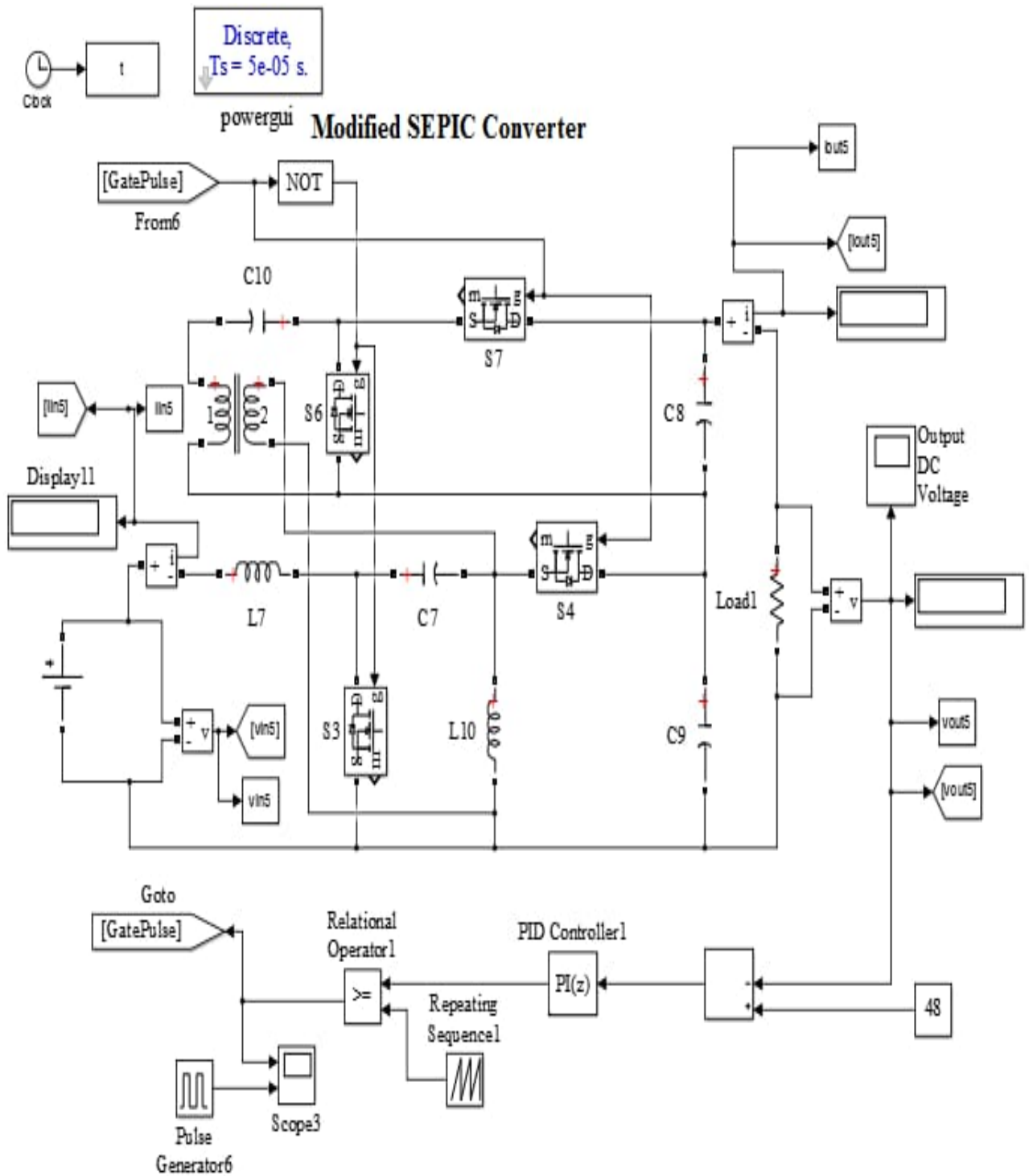
6.2 FUTURE SCOPE

A modified SEPIC converter can have several potential future scopes, including:

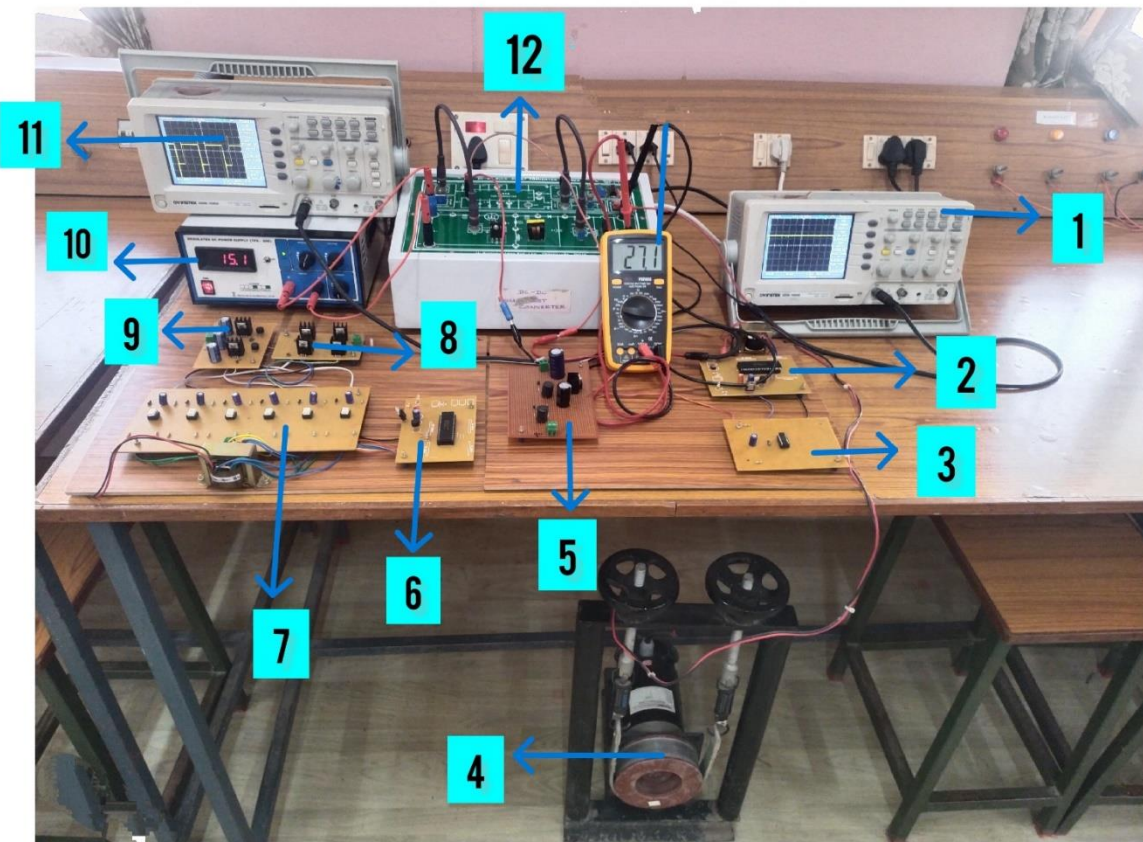
- **High power applications:** The SEPIC converter is typically used in low-power applications, but a modified SEPIC converter could potentially be designed for high power applications, such as electric vehicle charging stations or renewable energy systems.
- **Higher efficiency:** A modified SEPIC converter could be designed to increase its efficiency by reducing losses in the circuit, such as switching losses.
- **Multi-output converter:** A modified SEPIC converter can be designed to provide multiple outputs, which could be useful in applications that require different voltage levels.
- **Renewable energy systems:** A modified SEPIC converter can be used in renewable energy systems, such as solar or wind power, to convert the DC voltage generated by the panels or turbines to a voltage suitable for charging batteries.

APPENDICES

APPENDIX 1: MATLAB CIRCUIT



APPENDIX 2: SNAPSHOT OF THE PROPOSED CONVERTER



Component Names

- | | |
|----------------------|--------------------------|
| 1. Input Waveform | 7. Switching Control |
| 2. Gate Input Signal | 8. MOSFET Switches |
| 3. Gate Drive IC | 9. Bridge Rectifier |
| 4. BLDC Motor | 10. Voltage Regulator |
| 5. Driver Circuit | 11. Output Waveform |
| 6. Microcontroller | 12. Buck-Boost Converter |

APPENDIX 3: DATASHEETS

FAIRCHILD

A Schlumberger Company

IRF440-443/IRF840-843 MTM7N45/7N50 N-Channel Power MOSFETs, 8 A, 450 V/500 V

Power And Discrete Division

T-39-11

Description

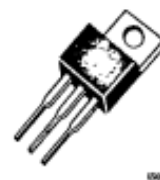
These devices are n-channel, enhancement mode, power MOSFETs designed especially for high voltage, high speed applications, such as off-line switching power supplies, UPS, AC and DC motor controls, relay and solenoid drivers.

- V_{GS} Rated at ± 20 V
- Silicon Gate for Fast Switching Speeds
- $I_{DS(on)}$, $V_{DS(on)}$, SOA and $V_{GS(th)}$ Specified at Elevated Temperature
- Rugged

TO-204AA



TO-220AB



IRF440
IRF441
IRF442
IRF443
MTM7N45
MTM7N50

IRF840
IRF841
IRF842
IRF843

Maximum Ratings

Symbol	Characteristic	Rating IRF440/442 IRF840/842 MTM7N50	Rating IRF441/443 IRF841/843 MTM7N45	Unit
V_{DSS}	Drain to Source Voltage	500	450	V
V_{DGR}	Drain to Gate Voltage $R_{GS} = 20$ k Ω	500	450	V
V_{GS}	Gate to Source Voltage	± 20	± 20	V
T_J , T_{Stg}	Operating Junction and Storage Temperature	-55 to +150	-55 to +150	°C
T_L	Maximum Lead Temperature for Soldering Purposes, 1/8" From Case for 5 s	275	275	°C

Maximum On-State Characteristics

		IRF440/441 IRF840/841	IRF442/443 IRF842/843	MTM7N45 MTM7N50	
$R_{DS(on)}$	Static Drain-to-Source On Resistance	0.85	1.1	0.8	Ω
I_D	Drain Current Continuous Pulsed	8 32	7 28	7 40	A

Maximum Thermal Characteristics

R_{JC}	Thermal Resistance, Junction to Case	1.0	1.0	0.83	°C/W
R_{JA}	Thermal Resistance, Junction to Ambient	60	60	60	°C/W
P_D	Total Power Dissipation at $T_C = 25^\circ C$	125	125	150	W

Notes

For information concerning connection diagram and package outline, refer to Section 7.

IRF440-443/IRF840-843

T-39-11

Electrical Characteristics ($T_C = 25^\circ\text{C}$ unless otherwise noted)

Symbol	Characteristic	Min	Max	Unit	Test Conditions
Off Characteristics					
$V_{(\text{BR})\text{DSS}}$	Drain Source Breakdown Voltage ¹			V	$V_{GS} = 0 \text{ V}, I_D = 250 \mu\text{A}$
	IRF440/442/840/842	500			
	IRF441/443/842/843	450			
$I_{\text{DS}}^{\text{SS}}$	Zero Gate Voltage Drain Current		250	μA	$V_{DS} = \text{Rated } V_{DSS}, V_{GS} = 0 \text{ V}$
			1000	μA	$V_{DS} = 0.8 \times \text{Rated } V_{DSS}, V_{GS} = 0 \text{ V}, T_C = 125^\circ\text{C}$
I_{GS}	Gate-Body Leakage Current			nA	$V_{GS} = \pm 20 \text{ V}, V_{DS} = 0 \text{ V}$
			± 100		
			± 500		
On Characteristics					
$V_{GS(\text{th})}$	Gate Threshold Voltage	2.0	4.0	V	$I_D = 250 \mu\text{A}, V_{DS} = V_{GS}$
$R_{DS(\text{on})}$	Static Drain-Source On-Resistance ²			Ω	$V_{GS} = 10 \text{ V}, I_D = 4.0 \text{ A}$
			0.85		
			1.10		
G_{fs}	Forward Transconductance	4.0		S (Ω)	$V_{DS} = 10 \text{ V}, I_D = 4.0 \text{ A}$
Dynamic Characteristics					
C_{iss}	Input Capacitance		1600	pF	$V_{DS} = 25 \text{ V}, V_{GS} = 0 \text{ V}$ $f = 1.0 \text{ MHz}$
C_{oss}	Output Capacitance		350	pF	
C_{rss}	Reverse Transfer Capacitance		150	pF	
Switching Characteristics ($T_C = 25^\circ\text{C}$, Figures 9, 10)					
$t_{d(on)}$	Turn-On Delay Time		35	ns	$V_{DD} = 220 \text{ V}, I_D = 4.0 \text{ A}$ $V_{GS} = 10 \text{ V}, R_{\text{GEN}} = 4.7 \Omega$ $R_{GS} = 4.7 \Omega$
t_r	Rise Time		15	ns	
$t_{d(off)}$	Turn-Off Delay Time		90	ns	
t_f	Fall Time		30	ns	
Q_g	Total Gate Charge		60	nC	$V_{GS} = 10 \text{ V}, I_D = 12 \text{ A}$ $V_{DD} = 400 \text{ V}$
Symbol Characteristic Typ Max Unit Test Conditions					
Source-Drain Diode Characteristics					
V_{SD}	Diode Forward Voltage IRF440/441/840/841 IRF442/443/842/843		2.0	V	$I_S = 8.0 \text{ A}; V_{GS} = 0 \text{ V}$
			1.9	V	$I_S = 7.0 \text{ A}; V_{GS} = 0 \text{ V}$
t_{rr}	Reverse Recovery Time	700		ns	$I_S = 8.0 \text{ A}; dI_S/dt = 100 \text{ A}/\mu\text{s}$

Notes

1. $T_J = +25^\circ\text{C}$ to $+150^\circ\text{C}$
2. Pulse test: Pulse width $\leq 80 \mu\text{s}$, Duty cycle $\leq 1\%$

MTM7N45/7N50

T-39-11

Electrical Characteristics ($T_C = 25^\circ\text{C}$ unless otherwise noted)

Symbol	Characteristic	Min	Max	Unit	Test Conditions
Off Characteristics					
$V_{(BR)DSS}$	Drain Source Breakdown Voltage ¹			V	$V_{GS} = 0 \text{ V}, I_D = 5.0 \text{ mA}$
	MTM7N50	500			
	MTM7N45	450			
I_{DSS}	Zero Gate Voltage Drain Current		0.25	mA	$V_{DS} = 0.85 \times \text{Rated } V_{DSS}$, $V_{GS} = 0 \text{ V}$
			2.5	mA	$V_{DS} = 0.85 \times \text{Rated } V_{DSS}$, $V_{GS} = 0 \text{ V}, T_C = 100^\circ\text{C}$
I_{GSS}	Gate-Body Leakage Current		± 500	nA	$V_{GS} = \pm 20 \text{ V}, V_{DS} = 0 \text{ V}$
On Characteristics					
$V_{GS(\text{th})}$	Gate Threshold Voltage	2.0	4.5	V	$I_D = 1.0 \text{ mA}, V_{DS} = V_{GS}$
		1.5	4.0	V	$I_D = 1.0 \text{ mA}, V_{DS} = V_{GS}$ $T_C = 100^\circ\text{C}$
$R_{DS(on)}$	Static Drain-Source On-Resistance ²		0.8	Ω	$V_{GS} = 10 \text{ V}, I_D = 3.5 \text{ A}$
$V_{DS(on)}$	Drain-Source On-Voltage ²		2.8	V	$V_{GS} = 10 \text{ V}, I_D = 3.5 \text{ A}$
			7.0	V	$V_{GS} = 10 \text{ V}, I_D = 7.0 \text{ A}$
			5.6	V	$V_{GS} = 10 \text{ V}, I_D = 3.5 \text{ A}$ $T_C = 100^\circ\text{C}$
g_{fs}	Forward Transconductance	4.0		S (S)	$V_{DS} = 10 \text{ V}, I_D = 4.0 \text{ A}$
Dynamic Characteristics					
C_{iss}	Input Capacitance		1800	pF	$V_{DS} = 25 \text{ V}, V_{GS} = 0 \text{ V}$ $f = 1.0 \text{ MHz}$
C_{oss}	Output Capacitance		350	pF	
C_{trs}	Reverse Transfer Capacitance		150	pF	
Switching Characteristics ($T_C = 25^\circ\text{C}$, Figures 9, 10)³					
$t_{d(on)}$	Turn-On Delay Time		60	ns	$V_{DD} = 25 \text{ V}, I_D = 3.5 \text{ A}$ $V_{GS} = 10 \text{ V}, R_{GEN} = 50 \Omega$ $R_{GS} = 50 \Omega$
t_r	Rise Time		150	ns	
$t_{d(off)}$	Turn-Off Delay Time		200	ns	
t_f	Fall Time		120	ns	
Q_g	Total Gate Charge		60	nC	$V_{GS} = 10 \text{ V}, I_D = 12 \text{ A}$ $V_{DD} = 400 \text{ V}$

Notes

1. $T_J = +25^\circ\text{C}$ to $+150^\circ\text{C}$

2. Pulse test: Pulse width $\leq 80 \mu\text{s}$, Duty cycle $\leq 1\%$

3. Switching time measurements performed on LEM TR-56 test equipment

IRF440-443/IRF840-843

MTM7N45/7N50

T-39-11

Typical Performance Curves

Figure 1 Output Characteristics

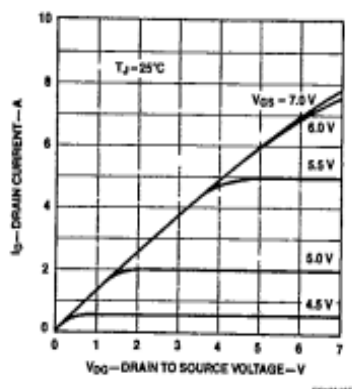


Figure 3 Transfer Characteristics

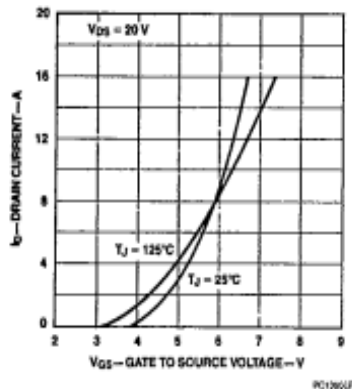


Figure 5 Capacitance vs Drain to Source Voltage

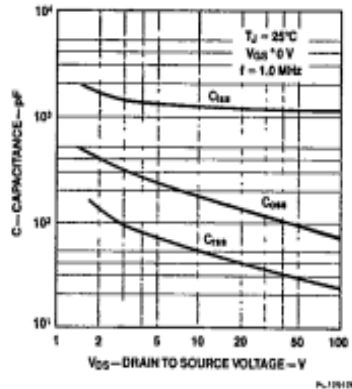


Figure 2 Static Drain to Source Resistance vs Drain Current

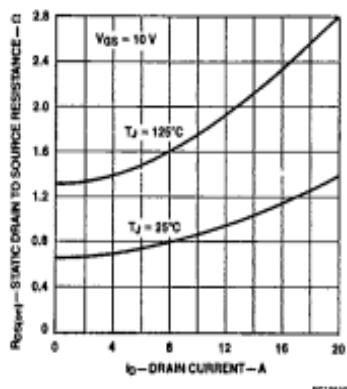


Figure 4 Temperature Variation of Gate to Source Threshold Voltage

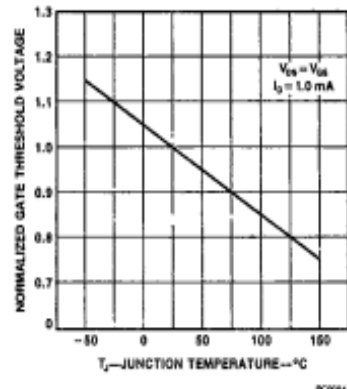
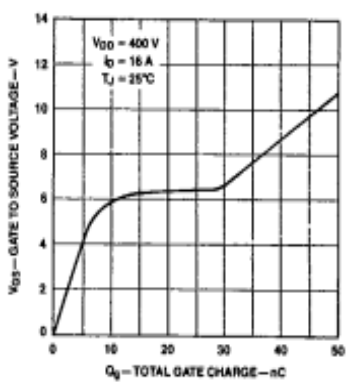


Figure 6 Gate to Source Voltage vs Total Gate Charge



IRF440-443/IRF840-843

MTM7N45/7N50

T-39-11

Typical Performance Curves (Cont.)

Figure 7 Forward Biased Safe Operating Area Curves

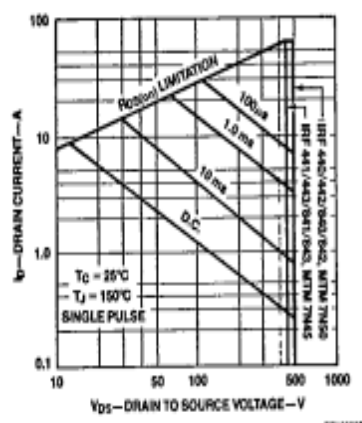
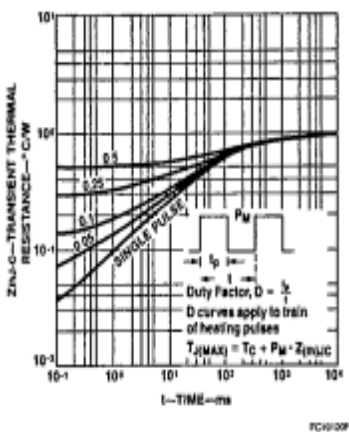


Figure 8 Transient Thermal Resistance vs Time



Typical Electrical Characteristics

Figure 9 Switching Test Circuit

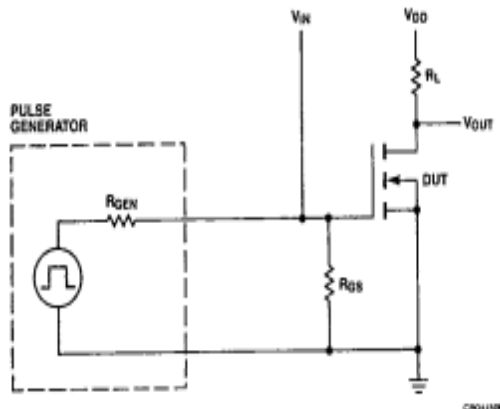
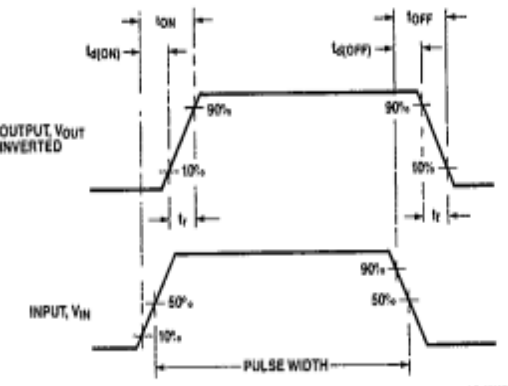


Figure 10 Switching Waveforms





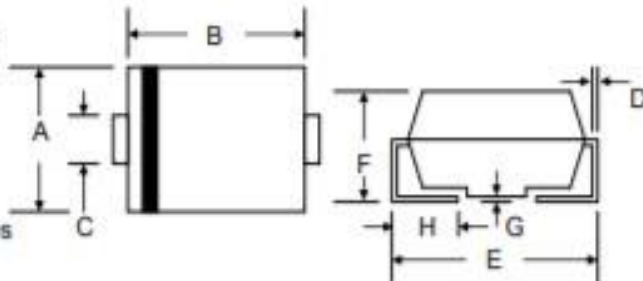
SR5150 – SR5200

5.0A HIGH VOLTAGE SURFACE MOUNT SCHOTTKY BARRIER DIODE



Features

- Low Forward Voltage
- Epitaxial Construction with Oxide Passivation
- Guard Ring for Transient and ESD Protection
- Surge Overload Rating to 125A Peak
- Low Power Loss
- Fast Switching
- Ideally Suited for Use in High Frequency SMPS, Inverters and As Free Wheeling Diodes



Mechanical Data

- Case: SMB/DO-214AA, Molded Plastic
- Terminals: Solder Plated, Solderable per MIL-STD-750, Method 2026
- Polarity: Cathode Band or Cathode Notch
- Marking: Device Code, See Page 3
- Weight: 0.093 grams (approx.)
- **Lead Free: For RoHS / Lead Free Version, Add "-LF" Suffix to Part Number, See Page 4**

SMB/DO-214AA		
Dim	Min	Max
A	3.30	3.94
B	4.06	4.70
C	1.91	2.11
D	0.152	0.305
E	5.08	5.59
F	2.13	2.44
G	0.051	0.203
H	0.76	1.27

All Dimensions in mm

Maximum Ratings @T_A=25°C unless otherwise specified

Characteristic	Symbol	SR5150	SR5200	Unit
Peak Repetitive Reverse Voltage	V _{RRM}			
Working Peak Reverse Voltage	V _{WRM}			
DC Blocking Voltage	V _{BR}	150	200	V
RMS Reverse Voltage	V _{RRMS}	105	140	V
Average Rectified Output Current (Note 1)	I _O		5.0	A
Non-Repetitive Peak Forward Surge Current 8.3ms Single Half Sine-Wave Superimposed on Rated Load (JEDEC Method)	I _{FSM}		125	A
Forward Voltage @I _F = 5.0A	V _{FM}		0.9	V
Peak Reverse Current @T _J = 25°C At Rated DC Blocking Voltage @T _J = 100°C	I _{RM}		0.2 5.0	mA
Typical Junction Capacitance (Note 2)	C _J		120	pF
Thermal Resistance, Junction to Ambient (Note 1)	R _{θJA}		70	°C/W
Thermal Resistance, Junction to Lead (Note 1)	R _{θJL}		18	°C/W
Operating and Storage Temperature Range	T _J , T _{STG}		-55 to +150	°C

Note: 1. Mounted on FR-4 PCB with 8.0 x 8.0mm copper pads.

2. Measured at 1.0 MHz and applied reverse voltage of 4.0V D.C.

SR5150 – SR5200

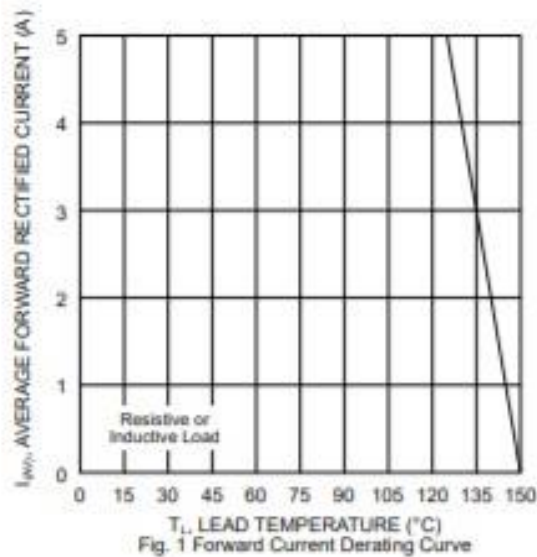


Fig. 1 Forward Current Derating Curve

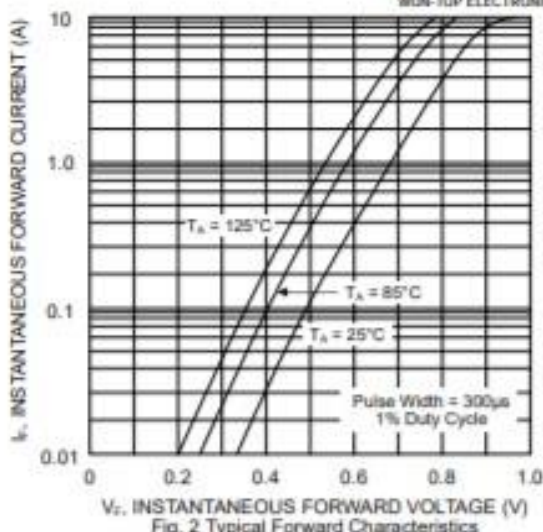


Fig. 2 Typical Forward Characteristics

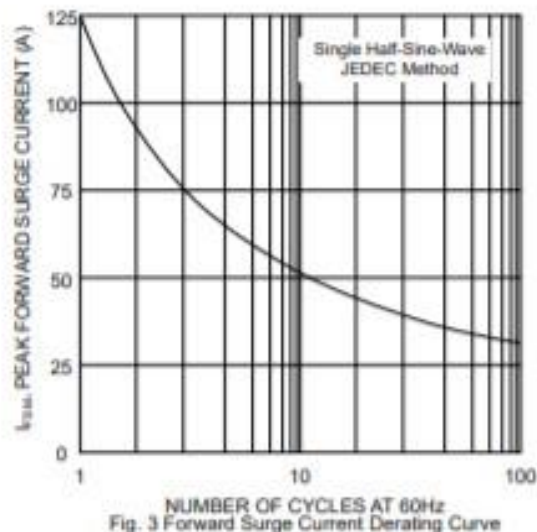


Fig. 3 Forward Surge Current Derating Curve

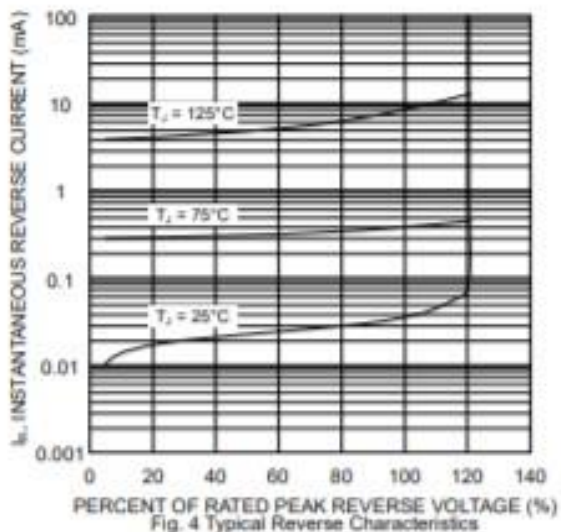


Fig. 4 Typical Reverse Characteristics

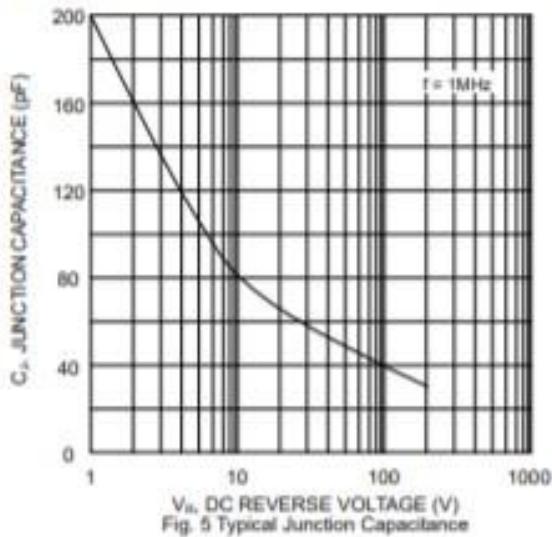


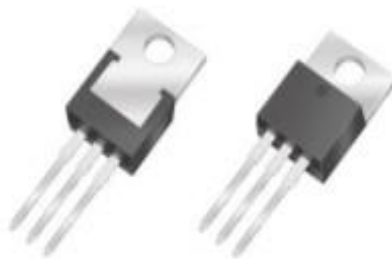
Fig. 5 Typical Junction Capacitance

20 Amperes High Power Schottky Barrier Rectifiers

Voltage : 40 to 250Volts

■Features

- For use in low voltage, high frequency inverters, free wheeling and polarity protection applications
- Low power loss, high efficiency
- High current capability, low forward voltage drop
- High surge capability
- Guardring for overvoltage protection
- Ultra high-speed switching
- Silicon epitaxial planar chip, metal silicon junction
- Lead-free parts meet environmental standards of MIL-STD-19500/228

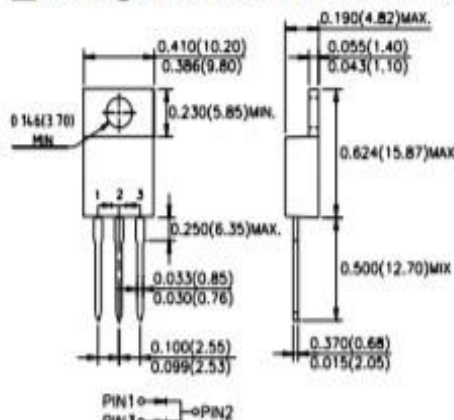


■Mechanical Data

Epoxy : UL94-V0 rated flame retardant
Case : JEDEC TO-220AB molded plastic body over
Terminals : Axial leads, Solderable per MIL-STD-202, Method 208 guaranteed
Polarity : Color band denotes cathode end
Mounting Position : Any
Weight : Approximated 2.25 gram
Package : 50pcs per Tube

■Package Dimensions

in inches(millimeters): TO-220AB



■Maximum Ratings And Electrical Characteristics

Rating at 25°C ambient temperature unless otherwise specified. Single phase, half wave, 60Hz, resistive or inductive load.
For capacitive load, derate current by 20%.

Parameter	Symbol	MBR2040CT	MBR2060CT	MBR20100CT	MBR20150CT	MBR20200CT	MBR20250CT	Unit
Marking Code		MBR2040CT	MBR2060CT	MBR20100CT	MBR20150CT	MBR20200CT	MBR20250CT	
Maximum Recurrent Peak Reverse Voltage	V _{RMS}	40	60	100	150	200	250	V
Maximum RMS Voltage	V _{RMS}	28	42	70	105	140	175	V
Maximum DC Blocking Voltage	V _{DC}	40	60	100	150	200	250	V
Maximum Forward Voltage@10A, T _A =25°C @10A, T _A =125°C @20A, T _A =25°C	V _F	0.70 0.57 0.84	0.79 0.70 0.95	0.81 0.71 0.95	0.87 0.77 1.0	0.90 0.80 1.0	0.95 0.85 -	V
Operating Temperature	T _J	-50 ~ +150						°C

Parameter	Conditions	Symbol	Min.	Typ.	Max.	Unit
Forward Rectified Current	See Fig.1	I _O			20	A
Forward Surge Current	8.3ms single half sine-wave superimposed on rate load (JEDEC method)	I _{FSM}			150	A
Reverse Current	V _R =V _{RMS} , T _A =25°C	I _R			0.1	mA
	V _R =V _{RMS} , T _A =125°C				10	
Thermal Resistance	Junction to ambient	R _{JA}		30		°C/W
Diode Junction Capacitance	f=1MHz and applied 4V DC reverse voltage	C _J		150		pF
Storage Temperature		T _{STG}	-50		+150	°C

■ Rated and Characteristic Curve

Fig. 1 - Forward Current Derating Curve

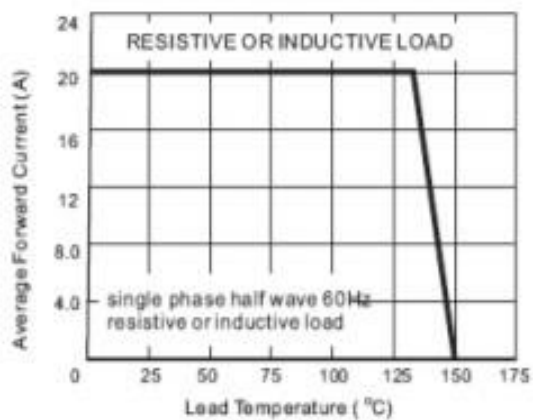


Fig. 3.1 - Typical Instantaneous Forward Characteristics

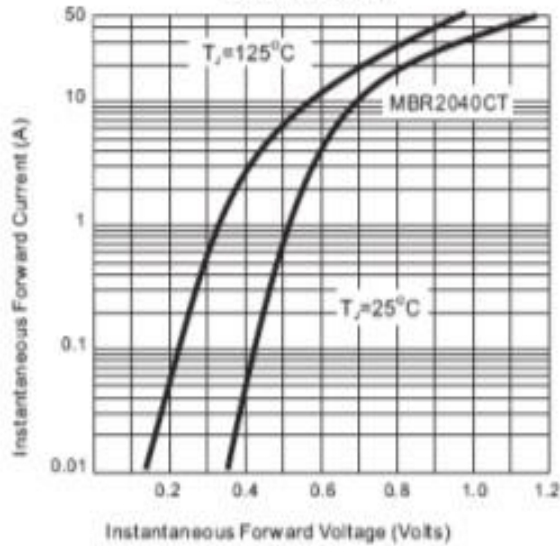


Fig. 3.3 - Typical Instantaneous Forward Characteristics

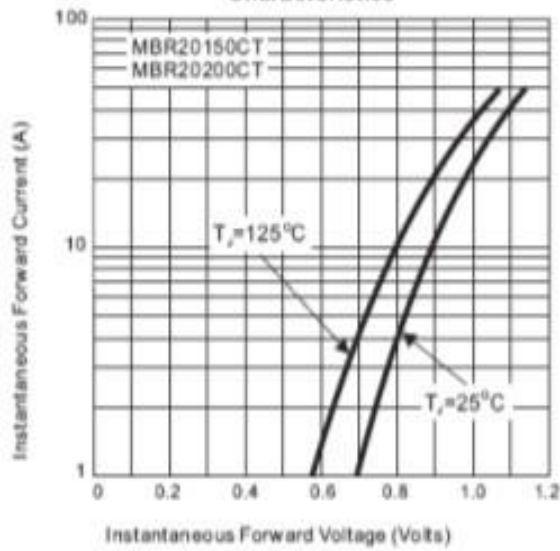


Fig. 2 - Maximum Non-Repetitive Peak Forward Surge Current

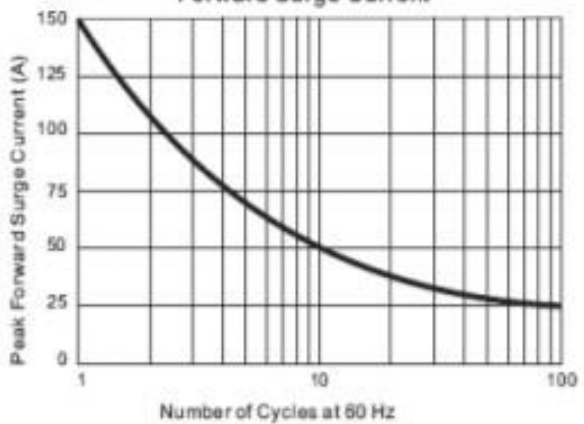


Fig. 3.2 - Typical Instantaneous Forward Characteristics

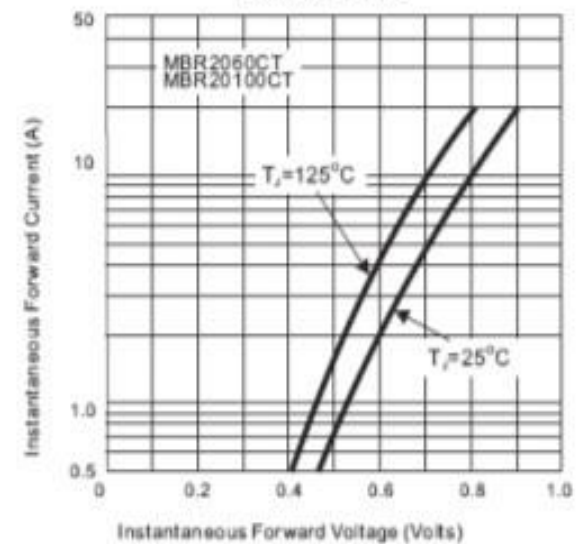
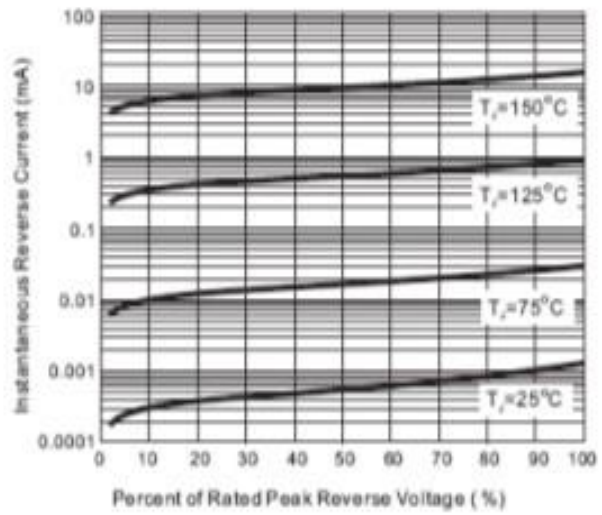


Fig. 4 - Typical Reverse Characteristics





July 2012

FAN7392

High-Current, High- and Low-Side, Gate-Drive IC

Features

- Floating Channel for Bootstrap Operation to +600V
- 3A/3A Sourcing/Sinking Current Driving Capability
- Common-Mode dv/dt Noise Cancelling Circuit
- 3.3V Logic Compatible
- Separate Logic Supply (V_{DD}) Range from 3.3V to 20V
- Under-Voltage Lockout for V_{CC} and V_{BS}
- Cycle-by-Cycle Edge-Triggered Shutdown Logic
- Matched Propagation Delay for Both Channels
- Outputs In-phase with Input Signals
- Available in 14-PDIP and 16-SOP (Wide) Packages

Applications

- High-Speed Power MOSFET and IGBT Gate Driver
- Server Power Supply
- Uninterrupted Power Supply (UPS)
- Telecom System Power Supply
- Distributed Power Supply
- Motor Drive Inverter

Description

The FAN7392 is a monolithic high- and low-side gate drive IC, that can drive high-speed MOSFETs and IGBTs that operate up to +600V. It has a buffered output stage with all NMOS transistors designed for high pulse current driving capability and minimum cross-conduction. Fairchild's high-voltage process and common-mode noise canceling techniques provide stable operation of the high-side driver under high dv/dt noise circumstances. An advanced level-shift circuit offers high-side gate driver operation up to $V_S=9.8V$ (typical) for $V_{BS}=15V$. Logic inputs are compatible with standard CMOS or LSTTL output, down to 3.3V logic. The UVLO circuit prevents malfunction when V_{CC} and V_{BS} are lower than the specified threshold voltage. The high-current and low-output voltage drop feature makes this device suitable for half- and full-bridge inverters, like switching-mode power supply and high-power DC-DC converter applications.

14-PDIP



16-SOP



Ordering Information

Part Number	Operating Temperature Range	Package	Packing Method
FAN7392N	-40°C to +125°C	14-PDIP	Tube
FAN7392M		16-SOP	Tube
FAN7392MX			Tape and Reel

Absolute Maximum Ratings

Stresses exceeding the absolute maximum ratings may damage the device. The device may not function or be operable above the recommended operating conditions and stressing the parts to these levels is not recommended. In addition, extended exposure to stresses above the recommended operating conditions may affect device reliability. The absolute maximum ratings are stress ratings only. $T_A=25^\circ\text{C}$ unless otherwise specified.

Symbol	Characteristics	Min.	Max.	Unit
V_B	High-Side Floating Supply Voltage	-0.3	625.0	V
V_S	High-Side Floating Offset Voltage	$V_B-25.0$	$V_B+0.3$	V
V_{HO}	High-Side Floating Output Voltage	$V_S-0.3$	$V_B+0.3$	V
V_{CC}	Low-Side Supply Voltage	-0.3	25.0	V
V_{LO}	Low-Side Floating Output Voltage	-0.3	$V_{CC}+0.3$	V
V_{DD}	Logic Supply Voltage	-0.3	$V_{SS}+25.0$	V
V_{SS}	Logic Supply Offset Voltage	$V_{CC}-25.0$	$V_{CC}+0.3$	V
V_{IN}	Logic Input Voltage (HIN, LIN and SD)	$V_{SS}-0.3$	$V_{DD}+0.3$	V
dV_S/dt	Allowable Offset Voltage Slew Rate		± 50	V/ns
P_D	Power Dissipation ^(1, 2, 3)	14-PDIP	1.6	W
		16-SOP	1.3	
θ_{JA}	Thermal Resistance	14-PDIP	75	$^\circ\text{C}/\text{W}$
		16-SOP	95	
T_J	Maximum Junction Temperature		+150	$^\circ\text{C}$
T_{STG}	Storage Temperature	-55	+150	$^\circ\text{C}$

Notes:

1. Mounted on 76.2 x 114.3 x 1.6mm PCB (FR-4 glass epoxy material).
2. Refer to the following standards:
JESD51-2: Integral circuits thermal test method environmental conditions, natural convection; and
JESD51-3: Low effective thermal conductivity test board for leaded surface-mount packages.
3. Do not exceed power dissipation (P_D) under any circumstances.

Recommended Operating Conditions

The Recommended Operating Conditions table defines the conditions for actual device operation. Recommended operating conditions are specified to ensure optimal performance to the datasheet specifications. Fairchild does not recommend exceeding them or designing to absolute maximum ratings.

Symbol	Parameter	Min.	Max.	Unit
V_B	High-Side Floating Supply Voltage	V_S+10	V_S+20	V
V_S	High-Side Floating Supply Offset Voltage	$6-V_{CC}$	600	V
V_{HO}	High-Side Output Voltage	V_S	V_B	V
V_{CC}	Low-Side Supply Voltage	10	20	V
V_{LO}	Low-Side Output Voltage	0	V_{CC}	V
V_{DD}	Logic Supply Voltage	$V_{SS}+3$	$V_{SS}+20$	V
V_{SS}	Logic Supply Offset Voltage	-5	5	V
V_{IN}	Logic Input Voltage	V_{SS}	V_{DD}	V
T_A	Operating Ambient Temperature	-40	+125	$^\circ\text{C}$

Electrical Characteristics

$V_{BIAS}(V_{CC}, V_{BS}, V_{DD})=15.0\text{V}$, $V_{SS}=\text{COM}=0\text{V}$ and $T_A=25^\circ\text{C}$, unless otherwise specified. The V_{IH} , V_{IL} , and I_{IN} parameters are referenced to V_{SS} and are applicable to the respective input leads: HIN, LIN, and SD. The V_O and I_O parameters are referenced to V_S and COM and are applicable to the respective output leads: HO and LO.

Symbol	Characteristics	Test Condition	Min.	Typ.	Max.	Unit
Low-Side Power Supply Section						
I_{QCC}	Quiescent V_{CC} Supply Current	$V_{IN}=0\text{V}$ or V_{DD}		40	80	μA
I_{QDD}	Quiescent V_{DD} Supply Current	$V_{IN}=0\text{V}$ or V_{DD}			10	μA
I_{PCC}	Operating V_{CC} Supply Current	$f_{IN}=20\text{kHz}$, rms, $V_{IN}=15\text{V}_{PP}$		430		μA
I_{PDD}	Operating V_{DD} Supply Current	$f_{IN}=20\text{kHz}$, rms, $V_{IN}=15\text{V}_{PP}$		300		μA
I_{SD}	Shutdown Supply Current	$S_D=V_{DD}$		120		μA
V_{CCUV+}	V_{CC} Supply Under-Voltage Positive-Going Threshold Voltage	$V_{IN}=0\text{V}$, V_{CC} =Sweep	7.7	8.8	9.9	V
V_{CCUV-}	V_{CC} Supply Under-Voltage Negative-Going Threshold Voltage	$V_{IN}=0\text{V}$, V_{CC} =Sweep	7.3	8.4	9.5	V
V_{CCUVH}	V_{CC} Supply Under-Voltage Lockout Hysteresis Voltage	$V_{IN}=0\text{V}$, V_{CC} =Sweep		0.4		V
Bootstrapped Supply Section						
I_{PBS}	Quiescent V_{BS} Supply Current	$V_{IN}=0\text{V}$ or V_{DD}		60	130	μA
I_{PBS}	Operating V_{BS} Supply Current	$f_{IN}=20\text{kHz}$, rms value		500		μA
V_{BSUV+}	V_{BS} Supply Under-Voltage Positive-Going Threshold Voltage	$V_{IN}=0\text{V}$, V_{BS} =Sweep	7.7	8.8	9.9	V
V_{BSUV-}	V_{BS} Supply Under-Voltage Negative-Going Threshold Voltage	$V_{IN}=0\text{V}$, V_{BS} =Sweep	7.3	8.4	9.5	V
V_{BSUVH}	V_{BS} Supply Under-Voltage Lockout Hysteresis Voltage	$V_{IN}=0\text{V}$, V_{BS} =Sweep		0.4		V
I_{LK}	Offset Supply Leakage Current	$V_B=V_S=600\text{V}$			50	μA
Input Logic Section (HIN, LIN, and SD)						
V_{IH}	Logic "1" Input Threshold Voltage	$V_{DD}=3\text{V}$	2.4			V
		$V_{DD}=15\text{V}$	9.5			V
V_{IL}	Logic "0" Input Threshold Voltage	$V_{DD}=3\text{V}$			0.8	V
		$V_{DD}=15\text{V}$			4.5	V
I_{IN+}	Logic Input High Bias Current	$V_{IN}=V_{DD}$		20	40	μA
I_{IN-}	Logic Input Low Bias Current	$V_{IN}=0\text{V}$			3	μA
R_{IN}	Logic Input Pull-Down Resistance		375	750		$\text{k}\Omega$
Gate Driver Output Section						
V_{OH}	High-Level Output Voltage ($V_{BIAS} - V_O$)	No Load ($I_O=0\text{A}$)			1.5	V
V_{OL}	Low-Level Output Voltage	No Load ($I_O=0\text{A}$)			200	mV
I_{O+}	Output High, Short-Circuit Pulsed Current ⁽⁴⁾	$V_O=0\text{V}$, $PW \leq 10\mu\text{s}$	2.5	3.0		A
I_{O-}	Output Low, Short-Circuit Pulsed Current ⁽⁴⁾	$V_O=15\text{V}$, $PW \leq 10\mu\text{s}$	2.5	3.0		A
V_{SS}/COM	$V_{SS}-\text{COM}/\text{COM}-V_{SS}$ Voltage Endurability		-5.0		5.0	V
$-V_S$	Allowable Negative V_S Pin Voltage for HIN Signal Propagation to HO			-9.8	-7.0	V

REFERENCES

REFERENCES

1. A.Anand and B.Singh. (2018)“Power Factor Correction in Cuk–SEPIC-Based Dual-Output Converter-Fed SRM Drive”, IEEE Transactions of Industrial Electronics, vol. 65, no. 2, pp. 1117-1127.
2. Al-Gabri AM, Fardoun AA and Ismail EH. (2015), “Bridgeless PFC modified SEPIC rectifier with extended gain for universal input voltage applications”, IEEE Transactions of Power Electronics, vol.30, no.8, pp.4272- 4282.
3. A.B.Jorgensen.(2015) “Derivation, Design and Simulation of ZETA converter”, IEEE TechRix.
4. Benlafkih Abdessamad, Krit Salah-ddine and Chafik Elidrissi Mohamed. (2013) “Design and Modeling of DC/DC Boost Converter for Mobile Device Applications”, International Journal of Science and Technology, Vol. 2, no. 5, pp. 394 – 401.
5. Bhim Singh, Vashit Bist, Chandra A, and Al-Haddad K. (2015)“Power Factor Correction in Bridgeless-Luo Converter fed BLDC Motor Drive”, IEEE Transactions of Industry Applications, Vol. 51, No. 2, pp. 1179 - 1188.
6. Dinesh Gopal, Umasankar Periasamy and Mohana Periyasamy. (2019)“Fuzzy and PID Controllers for Buck-Boost Converter Fed Bridgeless BLDC Motor over Cloud”, International Conference on Intelligent Data Communication Technologies and Internet of Things (ICICI), pp. 1328-1337.
7. Dong Liu, Yanbo Wang, Qi Zhang and Zhe Chen. (2020) “ZVZCS Full Bridge Three-Level DC/DC Converter with Reduced Device Count”, IEEE Transactions on Power Electronics, Vol. 35, no. 10, pp. 9965 – 9970.

8. Hamed Pourfarzad, Mohammad Saremi and Tohid Jalilzadeh. (2020) “An extended high-voltage-gain DC-DC converter with reduced voltage stress on switches/diodes”, Electrical Engineering, Springer Publications.
9. Hedra Saleeb, Khairy Sayed, Ahmed Kassem and Ramadan Mostafa. (2019) “Control and analysis of bidirectional interleaved hybrid converter with coupled inductors for electric vehicle applications”, Electrical Engineering, Springer Publications.
10. Jin Li, Jinjun Liu, Dushan Boroyevich, Paolo Mattavelli and Yaosuo Xue. (2019) “Three-level Active Neutral-Point-Clamped Zero-Current-Transition Converter for Sustainable Energy Systems”, IEEE Transactions on Power Electronics, Vol. 26, no. 12, pp. 3680 – 3693.
11. N.Kumarasabapathy & M. Ramasamy.(2020)“Modified isolated power factor correction Cuk-converter fed BLDC motor drive with Fuzzy Logic Controller for pumping applications” Journal of the Chinese Institute of Engineers, Vol. 43, no. 6, pp. 553 – 565.
12. M. Gildersleeve, H.P. Forghani-zadeh, and G.A. Rincon-Mora. (2020) “A Comprehensive Power Analysis and a Highly Efficient, Mode-Hopping DC-DC Converter”, IEEE Asia-Pacific Conference on ASIC, pp. 153-156.
13. Rodnei Regis de Melo, Fernando Lessa Tofoli, Sergio Daher and Fernando Luiz Marcelo Antunes. (2020) “Interleaved bidirectional DC - DC converter for electric vehicle applications based on multiple energy storage devices”, Electrical Engineering, Springer Publications.

14. Vaiyapuri Viswanathan & Seenithangom Jeevananthan. (2017) “Hybrid converter topology for reducing torque ripple of BLDC motor”, IET Power Electronics, Vol. 10, No. 12, pp. 1572-1587.
15. V. Bist and B. Singh. (2014) “PFC Cuk converter-fed BLDC motor drive”, IEEE Transactions on Power Electronics, Vol. 30, no. 2, pp. 871-887.

2023 IEEE Sponsored Third International Conference on
**Advances in Electrical, Computing, Communications
and Sustainable Technologies (ICAECT 2023)**

05 - 06, January 2023 | Bhilai, Chhattisgarh, India | www.icaect.com

Third Edition

Sponsored by



23CHEE 1066

Peer Reviewed

CERTIFICATE



Aswin Chenthilkumar

Department of EEE
Sri Ramakrishna Engineering College
Coimbatore, Tamil Nadu, India

for presenting the research paper entitled "Design and Implementation of Modified SEPIC, ZETA, Cuk, Quasi Z-Source Converter for BLDC Drive System – A Comparative Analysis" in the 2023 IEEE Sponsored Third International Conference on Advances in Electrical, Computing, Communications and Sustainable Technologies (ICAECT 2023) held at the Department of Electrical and Electronics Engineering, Shri Shankaracharya Technical Campus (SSTC), Bhilai, Chhattisgarh, India during 05 - 06, January 2023.

Dr. Shimpy Ralhan
Conference Chair

Dr. P. B. Deshmukh
General Chair

Ms. Jaya Mishra
President, SGES

Organized by



Electrical and Electronics Engineering
Shri Shankaracharya Technical Campus (SSTC)
Bhilai, Chhattisgarh, INDIA

Promotional Partner



2023 IEEE Sponsored Third International Conference on
**Advances in Electrical, Computing, Communications
and Sustainable Technologies (ICAECT 2023)**

05 - 06, January 2023 | Bhilai, Chhattisgarh, India | www.icaect.com

Third Edition

Sponsored by



23CHEE 1066

Peer Reviewed

CERTIFICATE



Giriprasath Uthayakumar

Department of EEE
Sri Ramakrishna Engineering College
Coimbatore, Tamil Nadu, India

This certificate is presented to

for presenting the research paper entitled "Design and Implementation of Modified SEPIC, ZETA, Cuk, Quasi Z-Source Converter for BLDC Drive System – A Comparative Analysis" in the 2023 IEEE Sponsored Third International Conference on Advances in Electrical, Computing, Communications and Sustainable Technologies (ICAECT 2023) held at the Department of Electrical and Electronics Engineering, Shri Shankaracharya Technical Campus (SSTC), Bhilai, Chhattisgarh, India during 05 - 06, January 2023.

Dr. Shimpy Ralhan
Conference Chair

Dr. P. B. Deshmukh
General Chair

Ms. Jaya Mishra
President, SGES

Organized by



Electrical and Electronics Engineering
Shri Shankaracharya Technical Campus (SSTC)
Bhilai, Chhattisgarh, INDIA

Promotional Partner



2023 IEEE Sponsored Third International Conference on
**Advances in Electrical, Computing, Communications
and Sustainable Technologies (ICAECT 2023)**

05 - 06, January 2023 | Bhilai, Chhattisgarh, India | www.icaect.com

Third Edition

Sponsored by



23CHEE 1066

Peer Reviewed

CERTIFICATE



Hariharan Babu

Department of EEE
Sri Ramakrishna Engineering College
Coimbatore, Tamil Nadu, India

This certificate is presented to

for presenting the research paper entitled "Design and Implementation of Modified SEPIC, ZETA, Cuk, Quasi Z-Source Converter for BLDC Drive System – A Comparative Analysis" in the 2023 IEEE Sponsored Third International Conference on Advances in Electrical, Computing, Communications and Sustainable Technologies (ICAECT 2023) held at the Department of Electrical and Electronics Engineering, Shri Shankaracharya Technical Campus (SSTC), Bhilai, Chhattisgarh, India during 05 - 06, January 2023.

Dr. Shimpy Ralhan
Conference Chair

Dr. P. B. Deshmukh
General Chair

Ms. Jaya Mishra
President, SGES

Organized by



Electrical and Electronics Engineering
Shri Shankaracharya Technical Campus (SSTC)
Bhilai, Chhattisgarh, INDIA

Promotional Partner



Design and Implementation of Modified SEPIC, ZETA, Cuk, Quasi Z-Source Converter for BLDC Drive System – A Comparative Analysis

Praveenkumar Chandran

Department of EEE

Sri Ramakrishna Engineering College
Coimbatore, Tamilnadu, India
praveenkumar.chandran@srec.ac.in,
www.orcid.org/0000-0002-7094-0714

Aswin Chenthilkumar

Department of EEE

Sri Ramakrishna Engineering College
Coimbatore, Tamilnadu, India
aswin.1903016@srec.ac.in

Giriprasath Uthayakumar

Department of EEE

Sri Ramakrishna Engineering College
Coimbatore, Tamilnadu, India
giriprasath.1903026@srec.ac.in

Hariharan Babu

Department of EEE

Sri Ramakrishna Engineering College
Coimbatore, Tamilnadu, India
hariharan.1903032@srec.ac.in

Abstract - For the system to work properly, it needs a suitable DC-DC converter. High output voltage and power, low harmonic distortion, low ripple content at both current and voltage, and high efficiency gain with fewer component requirements are just a few of the parameters for a good converter. A lot of the converters are made to meet some of the aforementioned requirements. With increased potential for BLDC drive-based Electric Vehicle (EV) applications, the converter chosen in this article is one that will be suitable for those applications. Before recommending a converter for a certain usage, its performance must be evaluated. Various converter topologies are considered. The validation process goes into great detail for the design topology, components used, equations created, loss calculations, and output performances. The majority of converters perform better than expected when choosing the right component values. Applications that work well are provided together with the findings of the converters and the related values.

Keywords - DC - DC converter, Modified SEPIC, ZETA, Quasi Z-Source, Cuk, BLDC and EV.

INTRODUCTION - A lot of research is presently being done in order to create a sustainable DC to DC converter for use in Electric Vehicle (EV) applications. In the 1890s, the first electric vehicle emerged. However, throughout the past century, major efforts have been made to improve performance control in order to complete the adoption of EVs in the automotive sector. This research also focuses on the controlling performance improvement of EVs using batteries. The majority of EV components include an energy storage system, a motor, converter topologies, and control schemes. The motors used in electric vehicle applications include the Induction Motor (IM), Synchronous Motor (SM), Switched Reluctance Motor (SRM), DC motor, and Brush-Less DC (BLDC) Motor. Among these motors, the IM and SM have some efficiency limitations, while the SRM and DC motor

causes sparking and acoustic noise, respectively. The motors discussed above have the following benefits over BLDC. It has a high power density, a strong starting torque, enhanced speed-torque characteristics, no acoustic noise or sparking, no winding on the rotary part, up to a 95% efficiency rate, and other benefits. So it makes sense to use a BLDC motor in electric vehicles. Extruder drive motors, actuators for industrial robots, feed drives for CNC machine tools, and linear and servo motors in the industrial field are further applications for BLDC motors. The following is a summary of the literature survey on selection converters. Fig. 1 displays the basic building blocks of the suggested approach.

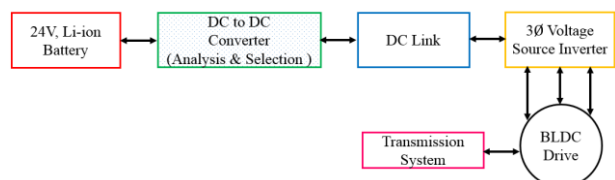


Fig. 1. General building blocks of the proposed approach

As suggested in [1], an SRM drive with a PFC-based converter combines Cuk and SEPIC converters. The SRM drive is commonly powered by a basic diode bridge rectifier, which draws peaky current with a low power factor and a high input-current THD. The next component is a sizable capacitor. The drawbacks include acoustic noise and having extra components. Power Factor Correction (PFC)-based Bridge-Less Luo (BL-Luo) converter-based BLDC motor drive was presented in [2]

One voltage sensor is used for the BLDC motor and PFC at ac mains speed control. The voltage follower control is used with a BL-Luo converter that is operating in the discontinuous inductor current mode. Because it permits low-frequency switching of the voltage source inverter for the motor's electronic commutation and lowers switching losses, a method of variable dc-link voltage is employed to control the BLDC motor's speed. The

suggested BLDC motor drive is designed to operate with better ac mains power quality and a range of speeds. A new single-phase AC-DC PFC bridgeless rectifier with a multiplier stage was invented in [3] with the goal of improving efficiency at low input voltage and reducing switch-voltage stress. To achieve an input current with a nearly unity power factor and minimum Total Harmonic Distortion (THD), the recommended architecture was designed to operate in Discontinuous Conduction Mode (DCM). The efficiency, THD, and power factor of a modified full-bridge SEPIC rectifier were evaluated using the architecture that was demonstrated. A modified Power Factor Correction Cuk Converter (PFCCC)-operated Voltage Source Inverter (VSI)-fed BLDC motor drive was developed in [4] for agricultural water pumping applications. To boost efficiency and PF and decrease the consequences of the system's low PF, PFC circuits are added to the AC input side of the water pumping system. Power Factor Correction (PFC) converters, such as the Zeta DC-DC converter in [5], are used to modify voltage to alter the speed of Permanent Magnet Brush-Less DC Motors (PMBLDCM).

The recommended drive's detailed design, modelling, and performance are shown for an air conditioner using a PMBLDC motor rated at 0.817 kW and 1500 rpm. A novel bidirectional interleaved hybrid converter using linked inductors (CIs) was proposed in [6] in order to maximise the performance of the power train in battery electric vehicles (BEVs). Realize the integration of the DC/DC converter and DC/AC inverter in the BEV power train, acting as a backup generator to send emergency power straight to the home, with good performance in every operating mode. It can lower system costs and volume while boosting effectiveness and dependability. The interleaving structure is used in this case to increase output power, minimise input current and output voltage ripple, reduce power loss, and increase efficiency. The use of CIs of energy storage inductors enhances the performance of the proposed converter. Supercapacitors (SCs) and batteries may be used in an EV design to deliver dependable and quick energy transfer, as discussed in [7].

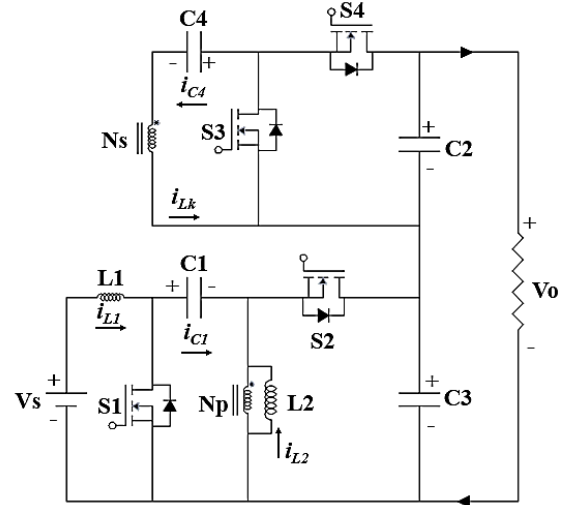
Power is moved between the abovementioned energy sources and the EV via a DC link coupled to a bidirectional interleaved dc-dc converter. The converter is investigated statistically and qualitatively, and as part of a comprehensive design process, a simple control system implementation is provided. A brand-new boost-based DC-DC converter without a transformer was proposed in study by [8]. Utilizing n levels of voltage multiplier cells and a charge-pump circuit (CPC), the voltage gain of the proposed converter was increased (VMC). By building a lab prototype with a power of 300 W, input and output voltages of 30 V and 310 V, respectively, and a switching frequency of 40 kHz, the performance of the converter is confirmed. The hybrid converter topology, also known as the SEPIC converter

fed three-level Neutral-Point-Clamped (NPC) inverter topology, was developed to eliminate torque ripples. The outcomes of this study led to the development of a system that, as detailed in [9], significantly reduces torque ripple when compared to a system based on a two-level NPC inverter.[10]

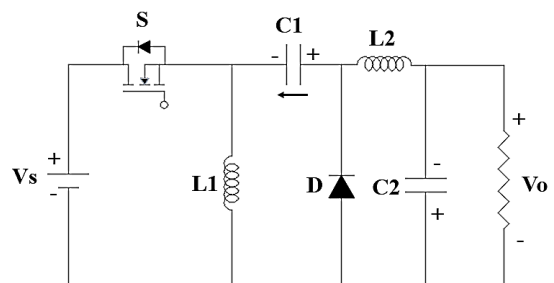
Identifying 2-kW BLDC-based EV applications with low ripple and high current output is the main objective of this work. The outcomes of several converter topologies' simulations are then contrasted. According to Modified SEPIC results, they are quite competitive with other converters. The rest of the paper is structured as follows: Output answers and reasons are presented after component design equations, simulated values, and design studies of various converter topologies. The paper then discusses ripple content analysis and comparative research.

II. DESIGN ANALYSIS OF CONVERTER TOPOLOGIES

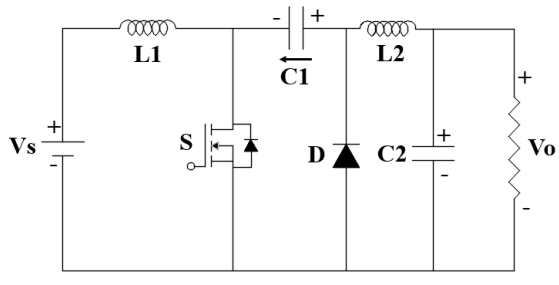
The design considerations and analysis for the investigation of suitable low ripple and high power converters, the following topologies are taken into account: Modified SEPIC, ZETA, cuk, and Quasi Z-source converters. These converters' circuit configurations are shown in Fig. 2.



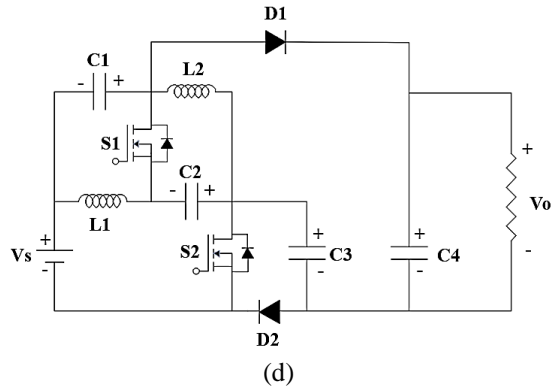
(a)



(b)



(c)



(d)

Fig. (2). Different converter topologies such as (a). Modified SEPIC topology (b). ZETA converter topology, (c). Cuk converter topology (d). Quazi Z-Source converter topology.

A. Modified SEPIC

The Modified SEPIC applications are high power, high current and static gain applications [11]. The Modified SEPIC consists of coupled inductor, leakage inductor \$L_1\$, magnetizing inductor \$L_2\$, four MOSFET switch \$S_1\$-\$S_4\$, two intermediate capacitors \$C_1\$ and \$C_4\$, output capacitor \$C_2\$ and \$C_3\$ and load resistor \$R\$. Fig. 2(a) displays the Modified SEPIC topology's circuit configuration.

Design Equations of Modified SEPIC

The Leakage and Magnetizing Inductance, \$L_1\$ & \$L_2\$ can be expressed as,

$$L = \frac{V_s D}{f_s * \Delta I_L} \quad (1)$$

For \$\Delta I_L\$, assuming for design calculation as 4.8% of \$I_{Load}\$.

$$L_1 = L_2 = \frac{24 * 0.67}{33.3 * 0.048} = 10 \text{ mH}$$

Where, \$V_s\$ - Source voltage (v), \$D\$ - duty cycle, \$f_s\$ - switching frequency (kHz), \$\Delta I_L\$ - change in load currents. The Intermediate capacitors, \$C_1\$ & \$C_4\$ can be calculated from the following equation.

$$C = \frac{V_o D}{R * f_s * \Delta I_C} \quad (2)$$

For \$\Delta V_C\$, assuming for design calculation as 2% of \$V_o\$.

$$C_1 = C_4 = \frac{48 * 0.67}{1 * 33.3 * 0.96} = 1000 \mu\text{F}$$

Where, \$V_o\$ - output voltage (v), \$D\$ - duty cycle, \$f_s\$ - switching frequency (kHz), \$\Delta V_C\$ - change in capacitive voltage. The Output filter capacitors, \$C_2\$ & \$C_3\$ are large enough to filter the output ripples.

$$C_2 = C_3 = 1200 \mu\text{F} \text{ (Kept as constant)}$$

Component values are derived and used in the Modified SEPIC simulation, which is shown in Table 1, based on the aforementioned formulae. The output response of Modified SEPIC is illustrated in Fig. 3. The input voltage, \$V_s\$, is specified as 24 volts, and the supply current, \$I_s\$, is 95A. The converter produced a 41.2v output voltage and a 41.12A output current. It is 1.99 times for the voltage conversion ratio. The converter has an efficiency rate of 73.8%.

Table 1. Values used in simulation of Modified SEPIC

S.No	Components	Values
1	Leakage Inductor, \$L_1\$	10 mH
2	Intermediate Capacitor, \$C_1\$ & \$C_4\$	1000 \$\mu\$F
3	Magnetizing Inductor, \$L_2\$	10 mH
4	Output Capacitor, \$C_2\$ & \$C_3\$	1200 \$\mu\$F
5	Switch x 4	MOSFET
6	Resistive Load, \$R\$	100 \$\Omega\$
7	Switching frequency, \$f_s\$	33 kHz

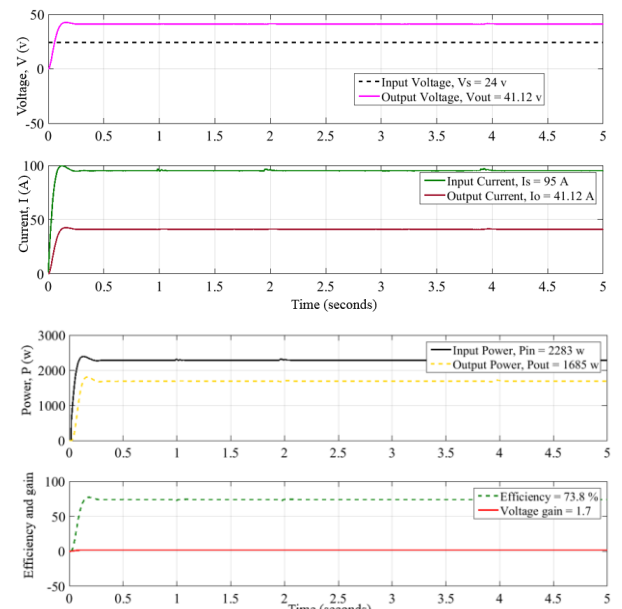


Fig. 3 Output response of Modified SEPIC

B. ZETA converter

The applications of ZETA converters are SMPS and automotive battery recharge from solar PV cells [12]. It consists of a single MOSFET switch, inductors L₁ and L₂, intermediate capacitors C₁, output capacitor C₂, and a load resistor R. Fig. 2(b) depicts the ZETA converter topology's circuit architecture.

Design Equations of ZETA converter

A straightforward Zeta converter design example is provided in the following section. The converter's input voltage is V_s = 24v, and its output must remain at 72v. The load resistance may be between 50 and 100Ω. The duty cycle D can be calculated by,

$$D = \frac{V_o}{V_d + V_o} \quad (4)$$

The inductors L₁ and L₂ can be obtained from the equation (13) and (14).

$$L_1 \geq \frac{(1-D)^2 * R_o}{2Df_s} \quad (5)$$

$$L_2 \geq \frac{(1-D)*R_o}{2f_s} \quad (6)$$

The sizing of capacitor C₁ can be expressed as,

$$C_1 \geq \frac{D*I_o}{\Delta V_{C1}*f_s} \quad (7)$$

Similarly, the sizing of capacitor C₂ can be expressed as,

$$C_2 \geq \frac{(1-D)*V_o}{8*\Delta V_{C1}*L_2*f_s^2} \quad (8)$$

Based on the above equations, component values are calculated and used in the simulation of ZETA converter, which is presented in Table 2.

Table 2. Components values used in simulation of ZETA converter

S.No	Components	Values
1	Inductors, L ₁ & L ₂	1.6 mH
2	Capacitor, C ₁	150 μF
3	Output Capacitor, C ₂	720 μF
4	Resistive Load, R	100 Ω
5	Switching frequency, f _s	25 kHz

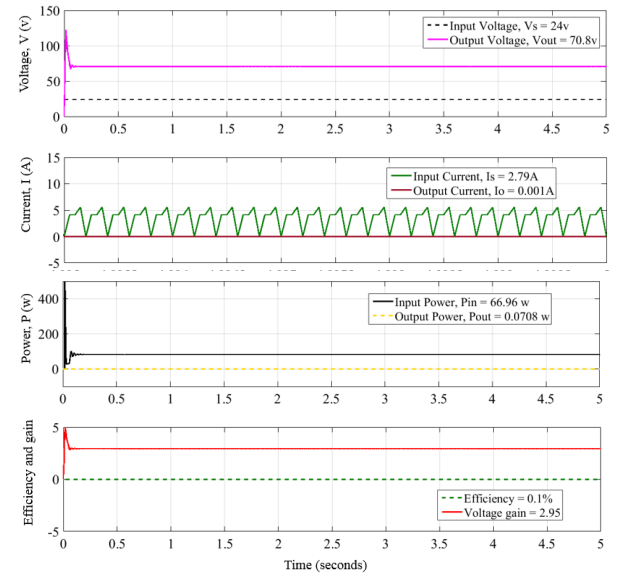


Fig. 4. Output response of ZETA converter

The output response of ZETA converter is illustrated in Fig. 4. The input voltage, V_s, is specified as 24 volts, and the supply current, I_s, is 2.79A. The converter produced a 70.8v output voltage and a 0.001A output current. It is 2.95 times for the voltage conversion ratio. The converter has an efficiency rate of 0.1%.

C. Cuk converter

In hybrid solar-wind energy systems, a Cuk converter is used as a regulator to maintain a constant output voltage where the input voltage is affected by the speed of the sun and wind. The voltage regulation for the DC application systems uses a Cuk converter [13] & [14]. The cuk converter consists of single MOSFET switch, inductors L₁ and L₂, intermediate storage capacitor C₁, output capacitor, C₂ and load resistor R. Fig. 2(c) depicts the Cuk converter's topology's circuit configuration.

Design Equations of CUK converter

The average value of input voltage is expressed as,

$$V_{in} = \frac{2\sqrt{2}V_s}{\pi} \quad (8)$$

The duty cycle ratio, D can be given as,

$$\frac{V_o}{V_s} = \frac{D}{1-D} \quad (9)$$

The input inductance, L₁ is calculated from,

$$L_1 = \frac{DV_{in}}{\Delta IL_1 f_s} \quad (10)$$

The output inductance, L_2 is calculated from,

$$L_2 = \frac{(1-D)DV_{dc}}{\Delta IL_2 f_s} \quad (11)$$

The intermediate capacitor, C_1 can be expressed as,

$$C_1 = \frac{DI_{dc}}{\Delta V_{C1} f_s} \quad (12)$$

The output capacitor, C_2 can be expressed as,

$$C_2 = \frac{I_{dc}}{\omega * \Delta V_{C2}} \quad (13)$$

Based on the above equations, component values are calculated and used in the simulation of Cuk converter, which is presented in Table 3.

Table 3. Values used in simulation of Cuk converter

S.No.	Components	Values
1	Inductors, L_1 & L_2	18 mH
2	Capacitor, C_1	200 μ F
3	Output Capacitor, C_2	720 μ F
4	Resistive Load, R	100 Ω

The output response of cuk converter is illustrated in Fig. 5. The input voltage, V_s , is specified as 24 volts, and the supply current, I_s , is 0.33 A. The converter produced a 23.1v output voltage and a 0.23A output current. It is 0.96 times for the voltage conversion ratio. The converter has an efficiency rate of 67.6%.

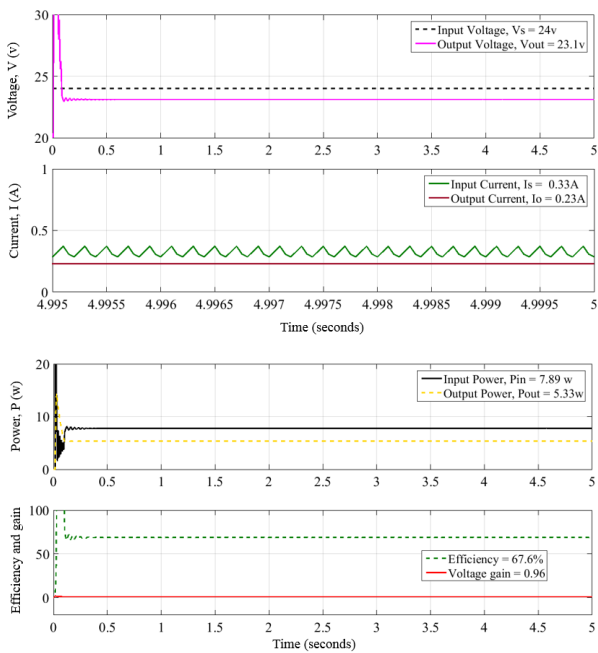


Fig. 5. Output response of Cuk converter

D. Quasi Z-source converter

The Quasi Z-source converter is compact, less expensive, and has a high efficiency [15]. It is used in wide range for high power with medium voltage applications.

It consists of two MOSFET switches, inductors L_1 and L_2 , diodes D_1 and D_2 , intermediate storage capacitor C_1 , C_2 , C_3 and C_4 and load resistor R. Fig. 2(d) depicts the circuit setup for the Quasi Z-source converter topology.

Design Equations of Quasi Z-source converter

The input inductor L_1 can be determined by,

$$L_1 \geq \frac{D(1-D)V_s}{\Delta i_{L1} f_s (1-2D)} \quad (14)$$

Similarly, inductor L_2 can be determined by,

$$L_2 \geq \frac{D(1-D)V_s}{\Delta i_{L2} f_s (1-2D)} \quad (15)$$

The Capacitors C_{1-4} value can be determined by,

$$C_1 \geq \frac{I_{L2}(1-D)}{\Delta V_{C1} f_s} \quad (16)$$

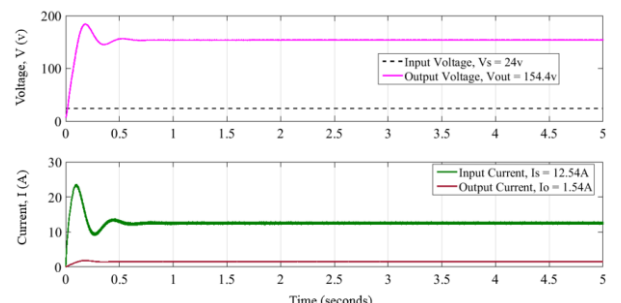
$$C_2 \geq \frac{I_{L2}(1-D)}{\Delta V_{C2} f_s} \quad (17)$$

$$C_3 \geq \frac{I_o}{\Delta V_{C3} f_s} \quad (18)$$

$$C_4 \geq \frac{I_o(1-D)}{\Delta V_{C4} f_s} \quad (19)$$

Table 4. Components values used in simulation of Quasi Z-source converter

S.No	Components	Values
1	Input Inductor, L_1	20 mH
2	Input Filter Capacitor, C_1	200 μ F
3	Magnetizing inductor, L_2	20 mH
4	Storage Capacitors, C_2 & C_3	650 μ F
5	Output Capacitor, C_4	1000 μ F
6	Resistive Load, R	100 Ω



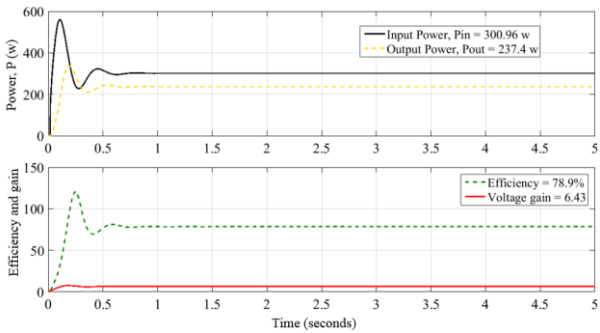


Fig. 6. Output response of Quazi Z-Source converter

The output response of Quazi Z-source converter is illustrated in Fig. 6. The input voltage, V_s , is specified as 24 volts, and the supply current, I_s , is 12.54 A.

The converter produced a 154.4v output voltage and a 1.54A output current. It is 6.43 times for the voltage conversion ratio. The converter has an efficiency rate of 78.9%.

III. COMPARATIVE ANALYSIS

For the purpose of comparison, all of the aforementioned converters are powered by 24v Li-ion batteries with a combined maximum current capacity of 110Ah.

The output responses are analysed in the subsequent part in order to determine the appropriate converter with the least output ripple and a high enough current to power 2kW BLDC motor-based electric vehicles. The output voltage that was obtained from the 24 volt battery supply is where the analysis begins.

Analysis of the voltage gain value is followed by consideration of input current ripple. The output load current is directly proportional to the input ripple voltage amplitude. At maximum output load, the input ripple amplitude reaches its maximum value. Additionally, the duty cycle of the converter affects the voltage ripple's amplitude. Without considerably raising the current stress and losses, one capacitor and one inductor can be added to provide the input current ripple cancellation. But by changing the remaining component values that are present in the converter topology, it is intended to reduce the current ripple. The input current ripple analysis is presented in Fig. 8 and output voltage waveform is given in Fig.7

In a DC circuit, output voltage ripple wastes energy and has a variety of unfavourable impacts, including component heating, noise and distortion, and the potential for poor operation of digital circuits. A voltage regulator and an electronic filter are both capable of

eliminating ripple and it is presented in Fig.9 and Fig.10. Many issues may result from a strong ripple current. For instance, the switching power supply may interpret this current draw as a fault condition if the ripple exceeds around 5% of the DC output current, in which case the over-current safety circuits may cause the supply to be shut down.

The load could lead to instability in the control loops if the pulse rate of the load is harmonically connected to the power supply switching frequencies. High ripple currents have the potential to severely overload switching supply outputs and accelerate their failure.

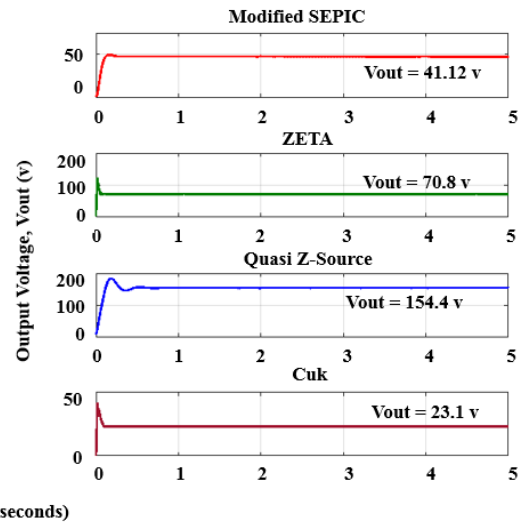


Fig. 7. Output voltage obtained from different converter topologies

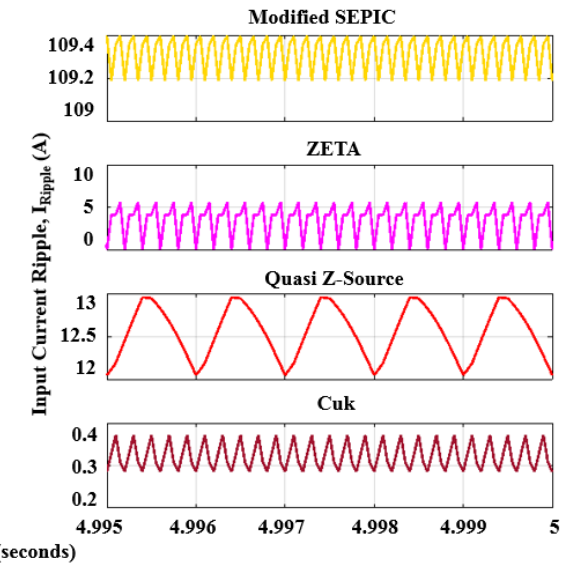


Fig. 8. Input current ripple analysis

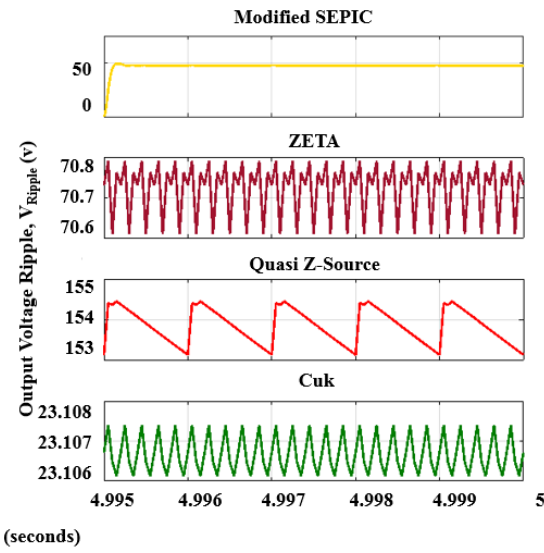


Fig. 9. Output voltage ripple analysis

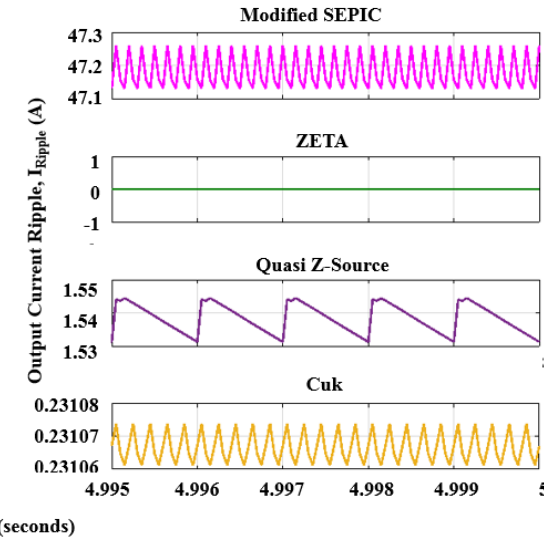


Fig. 10. Output current ripple analysis

The comparative analysis between the converter topologies values are tabulated in Table 5 and 6.

Table 5. Comparison of efficiency and voltage gain

	P_{in}, W	P_{out}, W	$\eta, \%$	n
Modified SEPIC	2283	1685	73.8	1.7
ZETA	66.96	0.0708	0.1	2.95
Cuk	7.89	5.33	67.6	0.96
Quasi Z-Source	300.96	237.4	78.9	6.43

IV. CONCLUSION

We conclude our analysis of a range of converter topology properties, including input and output voltage and current, ripple factor, efficiency, voltage gain, and component losses. The use of Modified SEPIC converters is suggested for BLDC-based EV applications.

The Modified SEPIC converter has a higher voltage gain ratio as a result. These are also incredibly tiny losses in comparison to other losses. The SEPIC's current output allows for a 2kW BLDC drive that can be used to power the vehicles.

Table 6. Comparative analysis of various converters

Input voltage, $V_s = 24\text{v}$ and Switching frequency, $f_s = 25 \text{ kHz}$

Converter topologies	Input current, A	Output voltage, v	Output current, A	Reduced Output ripple, %	No. of components	Applications
Modified SEPIC	95	41.12	41.12	0.30	11	High Power, High Current and Static Gain Applications
ZETA	2.79	70.8	0.001	0.40	6	SMPS and automotive battery recharge from solar PV cells
Cuk	0.33	23.1	0.23	0.34	6	as a regulator to maintain a constant output voltage
Quasi Z-Source	12.54	154.4	1.54	0.42	10	Wide range for high power with medium voltage applications

REFERENCES

- [1]. A. Anand and B. Singh, "Power Factor Correction in Cuk-SEPIC-Based Dual-Output-Converter-Fed SRM Drive", *IEEE Transactions of Industrial Electronics*, vol. 65, no. 2, pp. 1117-1127, Feb. 2018. <https://doi.org/10.1109/TIE.2017.2733482>.
- [2]. Bhim Singh, Vashit Bist, Chandra A, and Al-Haddad K "Power Factor Correction in Bridgeless-Luo Converter fed BLDC Motor Drive", *IEEE Transactions of Industry Applications*, Vol. 51, No. 2, pp. 1179 - 1188, 2015. <https://doi.org/10.1109/TIA.2014.2344502>.
- [3] Al-Gabri AM, Fardoun AA and Ismail EH, "Bridgeless PFC modified SEPIC rectifier with extended gain for universal input voltage applications", *IEEE Transactions of Power Electronics*, vol.30, no.8, pp.4272- 4282, 2015. <https://doi.org/10.1109/TPEL.2014.2351806>.
- [4]. N. Kumarasabapathy & M. Ramasamy, "Modified isolated power factor correction Cuk-converter fed BLDC motor drive with Fuzzy Logic Controller for pumping applications" *Journal of the Chinese Institute of Engineers*, Vol. 43, no. 6, pp. 553 - 565, July 2020. <https://doi.org/10.1080/02533839.2020.1777204>.
- [5]. Dinesh Gopal, Umasankar Periasamy and Mohana Periyasamy, "Fuzzy and PID Controllers for Buck-Boost Converter Fed Bridgeless BLDC Motor over Cloud", *International Conference on Intelligent Data Communication Technologies and Internet of Things (ICICI)*, pp. 1328-1337, Jan. 2019. https://doi.org/10.1007/978-3-030-03146-6_155.
- [6]. Hedra Saleeb, Khairy Sayed, Ahmed Kassem and Ramadan Mostafa, "Control and analysis of bidirectional interleaved hybrid converter with coupled inductors for electric vehicle applications", *Electrical Engineering*, Springer Publications, Nov. 2019. <https://doi.org/10.1007/s00202-019-00860-3>.
- [7]. Rodnei Regis de Melo, Fernando Lessa Tofoli, Sergio Daher and Fernando Luiz Marcelo Antunes, "Interleaved bidirectional DC - DC converter for electric vehicle applications based on multiple energy storage devices", *Electrical Engineering*, Springer Publications, May 2020. <https://doi.org/10.1007/s00202-020-01009-3>.
- [8]. Hamed Pourfarzad, Mohammad Saremi and Tohid Jalilzadeh, "An extended high-voltage-gain DC-DC converter with reduced voltage stress on switches/diodes", *Electrical Engineering*, Springer Publications, June 2020. <https://doi.org/10.1007/s00202-020-01040-4>.
- [9]. Vaiyapuri Viswanathan & Seenithangom Jeevananthan, "Hybrid converter topology for reducing torque ripple of BLDC motor", *IET Power Electronics*, Vol. 10, No. 12, pp. 1572-1587, 2017. <https://doi.org/10.1049/iet-pel.2015.0905>.
- [10]. Jin Li, Jinjun Liu, Dushan Boroyevich, Paolo Mattavelli and Yaosuo Xue, "Three-level Active Neutral-Point-Clamped Zero-Current-Transition Converter for Sustainable Energy Systems", *IEEE Transactions on Power Electronics*, Vol. 26, no. 12, pp. 3680 - 3693, Dec. 2011. <https://doi.org/10.1109/TPEL.2011.2161890>.
- [11]. Benlafkikh Abdessamad, Krit Salah-ddine and Chafik Elidrissi Mohamed, "Design and Modeling of DC/DC Boost Converter for Mobile Device Applications", *International Journal of Science and Technology*, Vol. 2, no. 5, pp. 394 - 401, May 2013.
- [12]. M. Gildersleeve, H.P. Forghani-zadeh, and G.A. Rincon-Mora, "A Comprehensive Power Analysis and a Highly Efficient, Mode-Hopping DC-DC Converter", *IEEE Asia-Pacific Conference on ASIC*, pp. 153-156, 2002.
- [13]. Dong Liu, Yanbo Wang, Qi Zhang and Zhe Chen, "ZVZCS Full Bridge Three-Level DC/DC Converter with Reduced Device Count", *IEEE Transactions on Power Electronics*, Vol. 35, no. 10, pp. 9965 - 9970, Feb. 2020. <https://doi.org/10.1109/TPEL.2020.2977227>.
- [14]. A.B. Jorgensen, "Derivation, Design and Simulation of ZETA converter", *IEEE TechRix*. <https://doi.org/10.36227/techrxiv.16732825.v1>.
- [15]. V. Bist and B. Singh, "PFC Cuk converter-fed BLDC motor drive", *IEEE Transactions on Power Electronics*, Vol. 30, no. 2, pp. 871-887, Mar. 2014. <https://doi.org/10.1109/TPEL.2014.2309706>.